bioRxiv preprint doi: https://doi.org/10.1101/2021.04.18.440372; this version posted April 19, 2021. The copyright holder for this preprint (which was not certified by peer review) is the author/funder, who has granted bioRxiv a license to display the preprint in perpetuity. It is made available under aCC-BY-NC-ND 4.0 International license.

Stabilisation of Antithetic Control via Molecular Buffering

Edward J. Hancock[1, 2] and Diego A. Oyarzún[3, 4]

[1)] *School of Mathematics and Statistics, The University of Sydney, NSW, 2006, Australia*

[2)] *Charles Perkins Centre, The University of Sydney, NSW, 2006, Australia*

[3)] *School of Informatics, The University of Edinburgh, United Kingdom*

[4)] *School of Biological Sciences, The University of Edinburgh, United Kingdom*

(Dated: 19 April 2021)

A key goal in synthetic biology is the construction of molecular circuits that robustly adapt to perturbations. Although many natural systems display perfect adaptation, whereby stationary molecular concentrations are insensitive to perturbations, its *de novo* engineering has proven elusive. The discovery of the antithetic control motif was a significant step toward a universal mechanism for engineering perfect adaptation. Antithetic control provides perfect adaptation in a wide range of systems, but it can lead to oscillatory dynamics due to loss of stability, and moreover, it can lose perfect adaptation in fast growing cultures. Here, we introduce an extended antithetic control motif that resolves these limitations. We show that molecular buffering, a widely conserved mechanism for homeostatic control in nature, stabilises oscillations and allows for near-perfect adaptation during rapid growth. We study multiple buffering topologies and compare their performance in terms of their stability and adaptation properties. We illustrate the benefits of our proposed strategy in exemplar models for biofuel production and growth rate control in bacterial cultures. Our results provide an improved circuit for robust control of biomolecular systems.

I. INTRODUCTION

Synthetic biology promises to revolutionise many sectors such as healthcare, chemical manufacture and materials engineering[7]. A number of such applications require precise control of biomolecular processes in face of environmental perturbations and process variability[22]. An important requirement in such control systems is *perfect adaptation*, a property whereby chemical concentrations remain insensitive to perturbations[20,23]. The molecular mechanisms that can produce perfect adaptation has been extensively studied in natural systems[3,14,20,23]. In these systems, perfect adaptation can be produced by a range of feedforward and feedback mechanisms[3,20]. Such natural systems have been shaped by evolutionary processes, but it remains unclear if they are sufficiently robust and tuneable for *de novo* engineering of perfect adaptation in synthetic circuits.

One approach to engineer perfect adaptation relies on the use of feedback control. As illustrated in Figure 1A, this strategy requires circuits that sense the output and act upon the inputs of a biomolecular process. The groundbreaking work by Briat and colleagues[1,4] identified *antithetic feedback* as a promising candidate for engineering perfect adaptation in living systems. Antithetic control involves a feedback mechanism with two molecular components that sequester and annihilate each other (see Figure 1B). It enables a system output to robustly follow an input signal and remain insensitive to various types of perturbations, akin to what integral feedback achieves in classic control engineering strategies[2].

The original antithetic control motif, however, has two weaknesses that can limit its applicability: it is often not effective when cells are growing rapidly, and the feedback mechanism can cause unwanted oscillations under a range of conditions[27]. Specifically, dilution effects caused by cell growth cause "leaky integration" - so called because integration is a form of memory and dilution causes that memory to leak over time[29]. This prevents perfect adaptation from occurring during rapid growth. Although in some motif configurations, the loss of perfect adaptation can be partly mitigated with a stronger feedback[29], in general the use of strong feedback results in the loss of stability and undesirable oscillations[27]. Such oscillations can be stabilised in specific motifs[15], and in more general cases the combination of antithetic control with classic Proportional-Integral-Derivative (PID) control has been shown to improve temporal regulation[5,9]. Yet to date, there is no general strategy to avoid oscillations and prevent the loss of adaptation during rapid growth.

Here we propose an extended antithetic control system that resolves the above limitations. We show that the addition of molecular buffers improves stability and suppresses undesirable oscillations, and moreover it can allow for near-perfect adaptation in fast growth regimes. Molecular buffering is a widespread regulatory mechanism in nature (e.g. ATP, calcium & pH buffers[17,21,32]) that has received modest attention in the literature as compared to other regulatory mechanisms. Recent work found that the combination of buffering and feedback is often critical for robust regulation[16,17]. Buffering has the ability to attenuate fast disturbances and stabilise feedback control[17] (see Figure 1C), and can also be essential for the control of multiple coupled outputs[18]. Here, we first show that a number of buffering topologies can stabilise the original antithetic control system and preserve perfect adaptation. We then show that buffering

bioRxiv preprint doi: https://doi.org/10.1101/2021.04.18.440372; this version posted April 19, 2021. The copyright holder for this preprint (which was not certified by peer review) is the author/funder, who has granted bioRxiv a license to display the preprint in perpetuity. It is made available under aCC-BY-NC-ND 4.0 International license.

can allow increased feedback strength or 'gain' without producing oscillations, which in turn reduces the steady state error even in fast growth conditions. To illustrate the utility of this new antithetic control strategy, we examine two case studies that involve the control of biofuel production and growth rate in microbes.

II. BACKGROUND

A. Perfect adaptation and antithetic control

Antithetic control employs a feedback mechanism with two molecular components that sequester and annihilate each other (see Figure 1B). In its most basic formulation, an antithetic system contains a two-species molecular process to be controlled, and a two-species antithetic controller. The two species of the controlled process (x_1 and x_2) can represent a variety of molecular systems, including e.g. mRNA and protein as in Figure 1A. The goal of the antithetic control system is to desensitise the steady state concentration of x_2 with respect to external perturbations. Such perturbations include, for example, insults of molecular species coming from upstream or downstream processes, changes in cellular growth conditions, or alterations to binding affinities between species.

In the absence of stochastic effects, the feedback system can be modelled by the ODEs:

$$\begin{aligned} \dot{x}_1 &= \theta_1 z_1 - \gamma_p x_1, \\ \dot{x}_2 &= k x_1 - \gamma_p x_2, \\ \dot{z}_1 &= \mu - \eta z_1 z_2 - \gamma_c z_1, \\ \dot{z}_2 &= \theta_2 x_2 - \eta z_1 z_2 - \gamma_c z_2, \end{aligned} \tag{1}$$

where z_1 and z_2 are the concentrations of species in the antithetic controller, and θ_1, k, and θ_2 are positive parameters representing first-order kinetic rate constants. The parameter μ describes a zero-order influx of controller species z_1, while η is a second-order kinetic rate constant. We further assume that molecular species are diluted by cellular growth, degraded by other molecular components, or consumed by downstream cellular processes, all of which we model as a first-order clearance with rate constant γ_p. The controller species z_1 and z_2, on the other hand, are assumed to be diluted by cellular growth with a rate constant γ_c.

In the absence of dilution effects ($\gamma_c = 0$), from the model in (1) we can write:

$$\dot{z}_1 - \dot{z}_2 = \mu - \theta_2 x_2,$$

which after integration becomes

$$z_1(t) - z_2(t) = \theta_2 \int_0^t \left(\frac{\mu}{\theta_2} - x_2(t') \right) dt'.$$

The above equation means that, if the system has a stable equilibrium, the steady state concentration of x_2 is

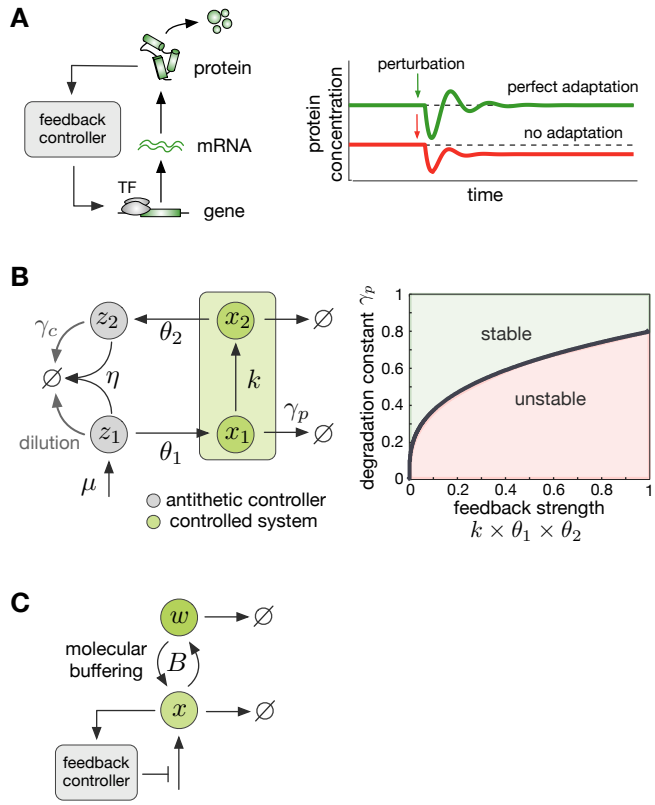

FIG. 1. Perfect adaptation and feedback control. **(A)** Schematic of a feedback system designed to achieve perfect adaptation in protein expression. Based on readouts of protein concentration, the controller modifies the activity of a transcription factor (TF). If the controller achieves perfect adaptation, steady state protein concentrations are robust to perturbations. **(B)** Left: the antithetic feedback controller, first proposed Briat *et al* in[4], can achieve perfect adaptation. In the presence of dilution ($\gamma_c \neq 0$), the antithetic controller does not achieve perfect adaptation. Right: conditions for stability in the case of a two-species system. The stability boundary is the condition in (2); the example was computed with fixed parameters $k = \theta_2 = \gamma_p = 1$. **(C)** In the example, molecular buffering provides a general mechanism to stabilize feedback control systems[17]. The buffer reversibly sequesters molecules of species x into an inactive form w.

$x_2 = \mu/\theta_2$, and hence independent of all model parameters except μ and θ_2. Therefore the antithetic control system displays perfect adaptation because the steady state of x_2 is robust to perturbations in parameters k, θ_1, θ_2 and η.

A caveat of antithetic feedback is that it can have a destabilising effect. When the controller species are not diluted ($\gamma_c = 0$), it can be shown that a parametric condition for stability is[27]:

$$\gamma_p^3 > \frac{k\theta_1\theta_2}{2}. \tag{2}$$

As shown by the stability diagram in Figure 1B, strong antithetic feedback can cause the system to lose perfect

bioRxiv preprint doi: https://doi.org/10.1101/2021.04.18.440372; this version posted April 19, 2021. The copyright holder for this preprint (which was not certified by peer review) is the author/funder, who has granted bioRxiv a license to display the preprint in perpetuity. It is made available under aCC-BY-NC-ND 4.0 International license.

adaptation and display oscillatory dynamics. Moreover, in the presence of dilution of the controller species ($\gamma_c > 0$), the antithetic controller is unable to produce perfect adaptation[27]. The adaptation error can be reduced with stronger feedback, for example by increasing the rate constants θ_1, k, or θ_2. Yet as mentioned above, stronger feedback can cause unwanted oscillations[27]. These caveats are particularly relevant in bioproduction applications that require fast culture growth[10,35].

B. Molecular buffering

Buffering is the use of molecular reservoirs to maintain the concentration of chemical species[17]. It is a widespread regulatory mechanism found across all domains of life, with common examples including pH, ATP and calcium buffering[21,32]. Molecular buffering can have a number of regulatory roles[17,18], including acting as a stabilising mechanism for other molecular feedback systems[17].

To provide a background on buffering models, we consider the simple case of a chemical species (x) that is subject to feedback regulation, as shown in Figure 1C. A general model for such process is:

$$\begin{aligned} \dot{x} &= \underbrace{p(x)}_{\substack{\text{production}\\ \text{with feedback}}} - \underbrace{\gamma_x x}_{\text{removal}} + \underbrace{g_w(w) - g_x(x)}_{\text{buffering}}, \\ \dot{w} &= \underbrace{g_x(x) - g_w(w)}_{\text{buffering}} - \underbrace{\gamma_w w}_{\text{removal}}, \end{aligned} \tag{3}$$

where w is a molecular buffer for the regulated species x, and $p(x)$ is a feedback-regulated production rate of x. The parameters γ_x and γ_w are first-order clearance rate constants of x and w, respectively. The terms g_w and g_x describe the reversible binding of species x and the buffer w. The steady state $(\bar{x}, \bar{w})$ occurs when production matches degradation (i.e. $p(\bar{x}) = \gamma_x \bar{x} + \gamma_w \bar{w}$) and conversion from x to w matches the reverse conversion plus removal (i.e. $g_w(\bar{w}) = g_x(\bar{x}) + \gamma_w \bar{w}$).

It can be shown that after linearisation and assuming that the buffering reactions rapidly reach quasi-equilibrium, the model (3) can be simplified to (see SI1):

$$(1+B)\Delta\dot{x} = -\underbrace{h\Delta x}_{\text{feedback}} - \underbrace{(\gamma_x + B\gamma_w)\Delta x}_{\text{removal}} \tag{4}$$

where $\Delta x = x - \bar{x}$ is the deviation of x from the steady state $\bar{x}$, $h = -\partial p/\partial x$ is the linearised feedback gain and B is the buffer equilibrium ratio:

$$B = \frac{\Delta w}{\Delta x}, \tag{5}$$

where $\Delta w = w - \bar{w}$ is the deviation of w from the steady state $\bar{w}$. The parameter B is buffer-specific and compares the change in the concentration of a regulated species, x, to the change in the concentration of a buffering species, w, when the buffering reactions are at quasi-equilibrium[17,18].

From (4) we observe that buffering slows down the rate of change of the output x by a factor of $(1+B)$. This slowed rate allows for attenuation of fast disturbances and stabilisation of unwanted oscillations[17] (see SI1). In the next section, we study the ability of buffering to stabilise oscillations in antithetic control systems.

III. BUFFERING CAN STABILISE ANTITHETIC INTEGRAL FEEDBACK

In this section we study a modified version of the antithetic feedback controller that includes buffering of its molecular components. We consider a number of architectures (Figure 2A) and identify those that suppress oscillations caused by the instability illustrated in Figure 1B.

To study the impact of buffering on the antithetic controller, we consider a mathematical model in which species z_1, z_2, and x_2 are buffered by molecules w_1, w_2, and w_x, respectively. For simplicity we use linear buffering reaction rates on the basis that the most important nonlinearity is the mutual annihilation of controller species z_1 and z_2[9]. As in Eq. (4), we assume that the buffers rapidly reach quasi-equilibrium to obtain the following extended model (see SI2):

$$\begin{aligned} \dot{x}_1 &= \theta_1 z_1 - \gamma_p x_1 \\ (1+B_x)\dot{x}_2 &= k x_1 - (\gamma_p + B_x\gamma_x) x_2 \\ (1+B_1)\dot{z}_1 &= \mu - \eta z_1 z_2 \\ (1+B_2)\dot{z}_2 &= \theta_2 x_2 - \eta z_1 z_2 \end{aligned} \tag{6}$$

where B_x, B_1 and B_2 are the equilibrium ratios for each buffer, and γ_x represents the degradation rate of buffer w_x. The extended model in (6) reduces to the original antithetic system in (1) if $B_x = 0$, $B_1 = 0$ and $B_2 = 0$.

In the extended antithetic controller, the parameters $(B_x, B_1, B_2, \gamma_x)$ are additional tuning knobs that can be used to shape the closed-loop dynamics. In Figure 2A we show the three considered buffering architectures. As a result, for rapid buffering we can compute the buffer concentrations as $w_2 = B_2 z_2$, $w_1 = B_1 z_1$ and $w_x = B_x x_2$.

We first show that buffered antithetic feedback preserves perfect adaptation. From (6) we write

$$(1+B_1)\dot{z}_1 - (1+B_2)\dot{z}_2 = \mu - \theta_2 x_2,$$

which after integrating becomes:

$$\begin{aligned} (1+B_1)z_1(t) - (1+B_2)z_2(t) \\ = \theta_2 \int_0^t \left(\frac{\mu}{\theta_2} - x_2(t') \right) dt'. \end{aligned}$$

bioRxiv preprint doi: https://doi.org/10.1101/2021.04.18.440372; this version posted April 19, 2021. The copyright holder for this preprint (which was not certified by peer review) is the author/funder, who has granted bioRxiv a license to display the preprint in perpetuity. It is made available under aCC-BY-NC-ND 4.0 International license.

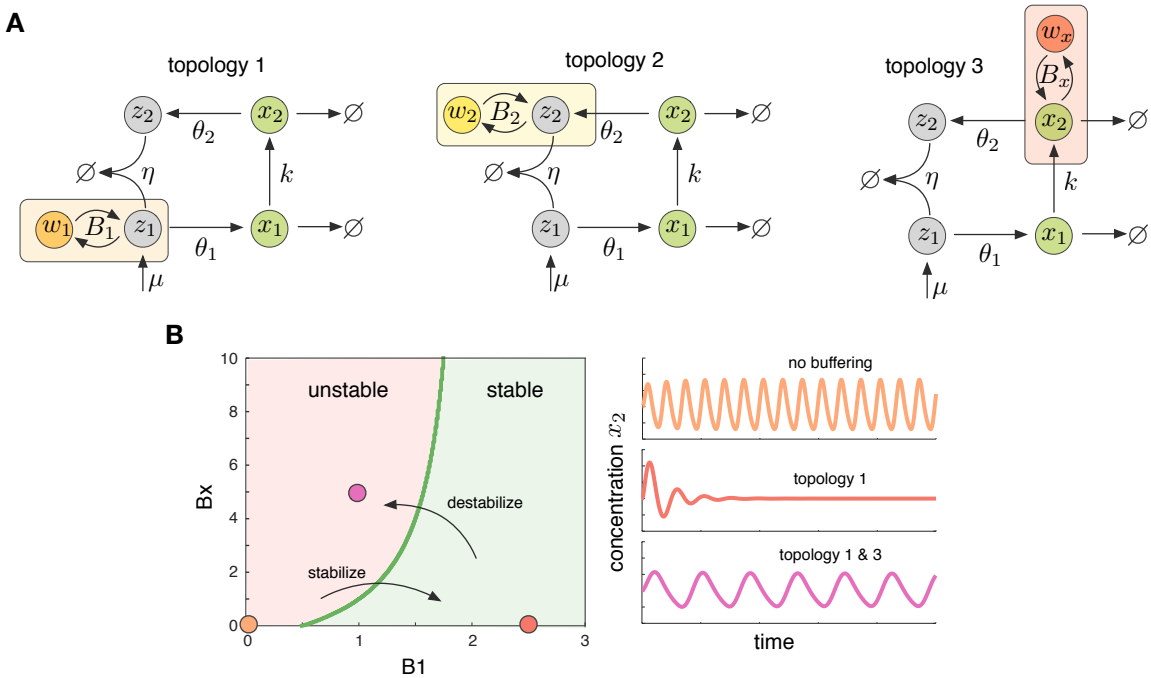

FIG. 2. **Buffering stabilizes antithetic feedback . (A)** Schematics of three buffered antithetic systems, without dilution ($\gamma_c = 0$); each topology includes buffering a specific molecular species. **(B)** Stability diagram for buffered topologies 1 and 3. The stability boundary corresponds to the condition in (7); topology 2 has no effect on stability. The time courses show simulations of the output species (x_2) for different topologies. Parameters are $\mu = 1$, $\theta_2 = 1$, $\gamma_p = 1$, $\eta = 100$ and $k = 1$. With z_1 and z_2 buffering, parameters are $\theta_1 = 3$, $B_1 = 0$ or $B_2 = 10$ and $B_2 = 0$ or $B_2 = 10$. With x_2 buffering, parameters are $\theta_1 = 1.5$, $\gamma_x = 1$ and $B_x = 0$ or $B_x = 20$.

The above integral ensures that if the system is stable then the steady state of x_2 is $x_2 = \mu/\theta_2$, hence independent of all parameters except μ and θ_2. The steady state of x_2 is thus robust to perturbations in the original parameters k, θ_1, θ_2, and η, as well as the additional parameters introduced by the buffering mechanism B_x, B_1, B_2, and γ_x. This means that the buffered antithetic feedback displays perfect adaptation as in the original formulation in Eq. (1).

As shown by the stability condition in (2), the original antithetic control system becomes oscillatory when the feedback gain is too strong or the degradation of x_1 and x_2 is too slow[27]. To analyse the stabilising role of buffering, we first consider the system in the absence of degradation of the w_x buffer (i. e. $\gamma_x = 0$). Assuming rapid buffering and strong integral binding (large η), we found that the system is stable when (see SI2):

$$\gamma_p^3 > \frac{\theta_1\theta_2 k}{(1+B_1)}\frac{1+B_x}{2+B_x}. \tag{7}$$

From the condition (7) we observe that increasing B_1 reduces the lower bound for γ_p and improves stability; this suggests that buffering of z_1 provides a route to suppress oscillations. The stability condition also shows that buffering of z_2 has no impact on stability, whereas buffering of x_2 can destabilise the system and produce oscillations. As shown in the stability diagram in Figure 2B, this finding means that molecular buffering in topologies 1 and 3 can counteract each other.

We next sought to identify variations of topology 3 that can ameliorate its destabilising effect. We found that degradation of the x_2 buffer (w_x) can indeed stabilise the closed-loop and eliminate the unwanted oscillations; this new topology is shown in Figure 3A. Under the same assumptions as condition (7) (rapid buffering and strong binding rate constant η), the stability conditions are (see SI3):

$$\gamma_p^3 > \frac{\theta_1\theta_2 k}{2+\left(1+\frac{\gamma_x}{\gamma_p}\right)B_x}\frac{1+B_x}{1+\frac{\gamma_x}{\gamma_p}B_x}. \tag{8}$$

Condition (8) reduces to the one in (7) if $\gamma_x = 0$ and there is no buffering of z_1 and z_2, i.e. $B_1 = B_2 = 0$.

As shown by the stability diagram in Figure 3B, topology 3 with degradation provides an effective solution to stabilise the closed-loop. The condition in (8) suggests that the ratio γ_x/γ_p has a key role in stability. Buffers with shorter half-lives (larger γ_x) tend to almost completely remove the instability, even for low buffer equilibrium ratios B_x. As we show in SI3, under the condition $\gamma_x/\gamma_p > 1/3$, increases in B_x tend to stabilise the closed-loop. This includes the important case where both x_2 and its buffer are degraded at the same rate, i.e. $\gamma_x = \gamma_p$. For large values of B_x, the stabilisation effect is even stronger and becomes independent of the

bioRxiv preprint doi: https://doi.org/10.1101/2021.04.18.440372; this version posted April 19, 2021. The copyright holder for this preprint (which was not certified by peer review) is the author/funder, who has granted bioRxiv a license to display the preprint in perpetuity. It is made available under aCC-BY-NC-ND 4.0 International license.

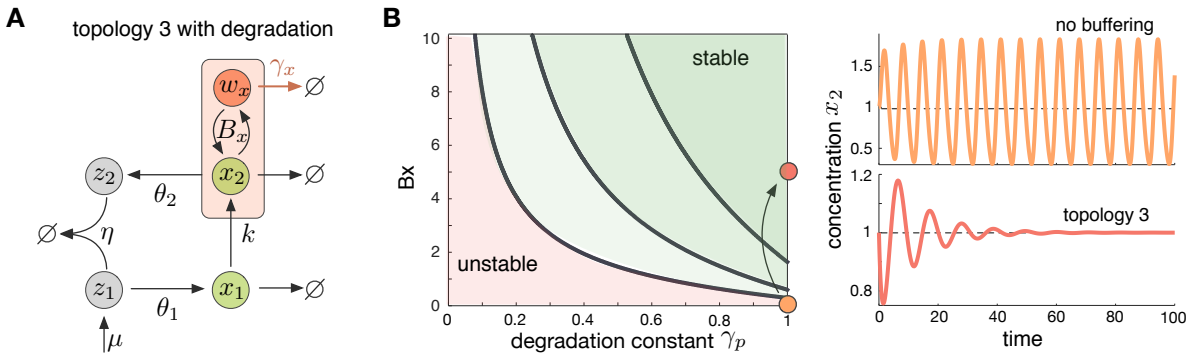

FIG. 3. **Stabilizing effect of topology 3 with degradation. (A)** We revisit topology 3 with degradation of the buffer with degradation rate constant γ_x. **(B)** Stability diagram for increasing values of the degradation rate constant $\gamma_x = \{0.5, 1, 2\}$; the stability boundary corresponds to the condition in (8). Time courses are simulations of the output species (x_2) for two representative cases. Parameter values are $\mu = 1$, $\theta_1 = 2$, $\theta_2 = 1$, $\gamma_p = 1$, $\eta = 100$ and $k = 1$. For the case of buffering $B_x = 20$ and $\gamma_x = 1$.

half-life of w_x. We found a similar stabilisation effect in systems with x_1 buffering that include degradation of the buffer (see SI4).

IV. ACHIEVING NEAR PERFECT ADAPTATION IN FAST GROWTH

In this section we investigate the effect of buffering on antithetic control with dilution. It is well-known that dilution by cell growth can disrupt perfect adaptation in the original antithetic control system[1], and thus here we explore the impact of dilution in the proposed topologies with molecular buffering. To study the effect of dilution, we modify (6) to include dilution terms for the control species z_1 and z_2, as well as the buffer for z_1:

$$\begin{aligned} \dot{x}_1 &= \theta_1 z_1 - \gamma_p x_1 \\ (1+B_x)\dot{x}_2 &= k x_1 - (\gamma_p + B\gamma_x) x_2 \\ (1+B_1)\dot{z}_1 &= \mu - \eta z_1 z_2 - \gamma_c (1+B_1) z_1 \\ \dot{z}_2 &= \theta_2 x_2 - \eta z_1 z_2 - \gamma_c z_2 \end{aligned} \tag{9}$$

where γ_c represents the dilution rate constant of the control species z_1, z_2 and buffer species at z_1. As in the previous model in (6), the model (9) can be obtained under the assumption of rapid equilibrium of the buffering reaction. Moreover, we further assume that dilution of x_1 and x_2 and the buffer at x_2 can be lumped into their first-order degradation rates.

A. Topology 3

For the case of dilution with a single buffer at x_2, we set $B_1 = 0$ in (9). The resulting steady state is (see SI5)

$$x_2 = \left(\frac{\mu}{\theta_2}\right) \times \left(\frac{1}{1+\Omega_x^{-1}}\right), \tag{10}$$

where

$$\Omega_x = \frac{\alpha}{\gamma_c \left(1 + B_x \frac{\gamma_x}{\gamma_p}\right)} \tag{11}$$

and $\alpha = \theta_1 \theta_2 k / \gamma_p^2$. The second term in (10) is always smaller than unity. Therefore the steady state of the output is $x_2 < \mu/\theta_2$ and the system loses perfect adaptation. Moreover, the deviation of the steady state of x_2 from the reference point μ/θ_2 is (see SI5):

$$\frac{x_{2n} - x_2}{x_{2n}} = \frac{1}{1+\Omega_x} \tag{12}$$

where $x_{2n} = \mu/\theta_2$ is the reference input. Increases to B_x, γ_c or γ_x in (12) thus amplify the steady state error, while increases to the feedback strength $k \times \theta_1 \times \theta_2$ brings the system closer to perfect adaptation. We further obtained parametric conditions for stability (see SI5):

$$\begin{aligned} \Omega_x &< \left(1 + \frac{\gamma_c}{\gamma_p}\right)(1+A)\left(\frac{\gamma_p}{\gamma_c} + A^{-1}\right) \\ A &= \frac{1 + B_x \frac{\gamma_x}{\gamma_p}}{1 + B_x}. \end{aligned} \tag{13}$$

Taken together, the relations in (12)–(13) define an upper bound for the best possible steady state error. Specifically, in (12) we see that stronger feedback gain can increase Ω_x and so reduce the steady state error. Buffering of x_2 tends to stabilise the oscillations and, at the same time, allows the steady state error to be reduced by stronger feedback gain, without the risk of instability observed in the original formulation. This phenomenon is illustrated in Figure 4A, which shows the stability condition (13). Notably, we observe that increasing B_x improves stability only in regions for low and high values of γ_x, and not intermediate values. Figure 4B shows simulations of the stabilising effect of molecular buffering for the case of $\gamma_x = 10$, which enables a decrease of

bioRxiv preprint doi: https://doi.org/10.1101/2021.04.18.440372; this version posted April 19, 2021. The copyright holder for this preprint (which was not certified by peer review) is the author/funder, who has granted bioRxiv a license to display the preprint in perpetuity. It is made available under aCC-BY-NC-ND 4.0 International license.

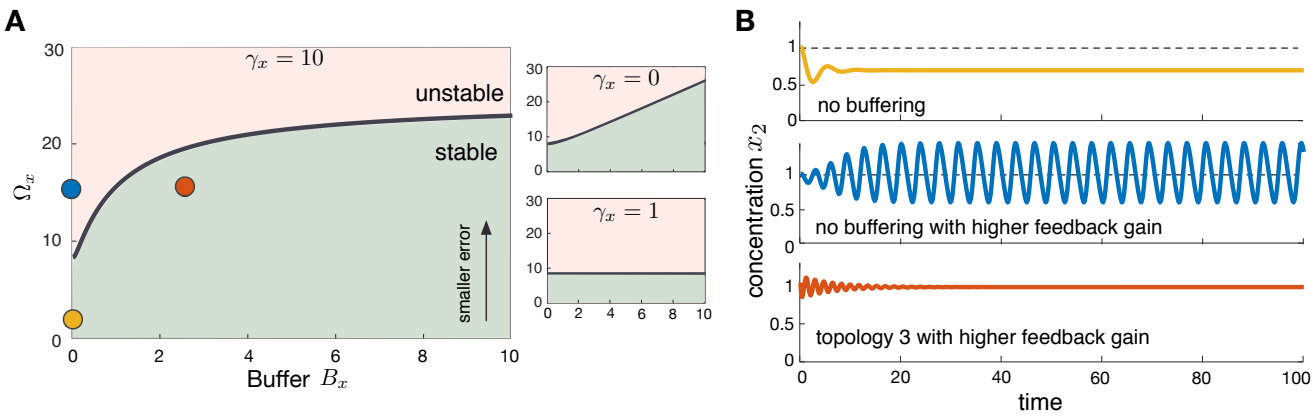

FIG. 4. **Adaptation in topology 3 with dilution. (A)** Stability condition in (13) for dilution rate constant $\gamma_c = 1$, $\gamma_p = 1$. **(B)** Simulation with varying feedback gain $\theta_1 = 2, 15, 400$ (from top) and topology 3 buffering ($B_x = 0, 2.5$). In all simulations the model parameters are $k = 1$, $\theta_2 = 1$, and $\gamma_p = 1$, $\gamma_c = 1$ and $\gamma_x = 10$.

steady state error by means of stronger feedback gain. We also found that topology 3 improves stability even without buffer degradation ($\gamma_x = 0$), unlike the case when there is no dilution in (7) and Figure 2.

B. Topology 1

We found that buffering at z_1 can similarly reduce steady state error via increases to the feedback gain. However, unlike Topology 3, this compensatory effect only occurs for systems that utilise slow buffers. To examine this result in detail, we set $B_x = 0$ in (9) and compute the resulting steady state (see SI7):

$$x_2 = \left(\frac{\mu}{\theta_2}\right) \times \left(\frac{1}{1+\Omega_1^{-1}}\right) \tag{14}$$

where

$$\Omega_1 = \frac{\alpha}{\gamma_c(1+B_1)} \tag{15}$$

and $\alpha = \theta_1\theta_2 k/\gamma_p^2$. As in the previous case, the steady state satisfies $x_2 < \mu/\theta_2$ and thus the system loses perfect adaptation (see Figure 5). Moreover, in this case the steady state error is (see SI7):

$$\frac{x_{2n} - x_2}{x_{2n}} = \frac{1}{1+\Omega_1} \tag{16}$$

where $x_{2n} = \mu/\theta_2$ is the reference input. Increasing B_1 or γ_c in (16) increases the steady state error, while increasing the feedback strength $k\theta_1\theta_2$ brings the system closer to perfect adaptation. Assuming rapid buffering, the conditions for stability is (see SI7):

$$\Omega_1 < 2\frac{\gamma_p}{\gamma_c}\left(1+\frac{\gamma_c}{\gamma_p}\right)^2. \tag{17}$$

From condition (17) we observe that rapid z_1 buffering results in no net change to the steady state error; this effect can be observed in simulations in Figure 5A. Increases to B_1 enable higher gain feedback without destabilising the system, but they also worsens the steady state error in (16) and the two effects cancel each other.

As we show in SI8, slow buffering of z_1 also enables an increase in the feedback gain without producing oscillations, which is similarly at the expense of an increased adaptation error. But in this case the net effect of buffering and increased feedback gain is positive and there is an overall reduction of the adaptation error, as shown in the simulations in Figure 5B.

V. CASE STUDIES

A. Model for biofuel production

To illustrate the potential of the proposed control topologies, here we employ an existing model for biofuel production that incorporates antithetic control[6] (see also[12]), shown in Figure 6A. The synthetic system produces biofuel from sugars through a metabolic pathway. The biofuel product can be toxic to the cell and so efflux pump proteins are expressed to remove the toxic metabolic product. However, at large concentrations the efflux protein pump can also be toxic. A feedback mechanism can help robustly regulate these two competing toxic products. The antithetic feedback mechanism senses the biofuel concentration to control the expression of efflux pump protein. An increase in the pump protein then reduces the biofuel concentration, completing the loop. Stability is known to be a major issue for the system, as it susceptible to oscillation for large η, which is the typical design case[6].

The extended model of the biofuel circuit with anti-

bioRxiv preprint doi: https://doi.org/10.1101/2021.04.18.440372; this version posted April 19, 2021. The copyright holder for this preprint (which was not certified by peer review) is the author/funder, who has granted bioRxiv a license to display the preprint in perpetuity. It is made available under aCC-BY-NC-ND 4.0 International license.

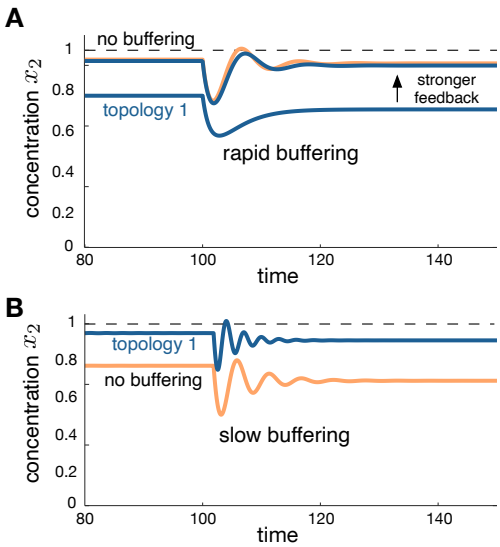

FIG. 5. Adaptation in topology 1 with dilution. **(A)** Rapid buffering increases the adaptation error while rapid buffering with stronger feedback is identical to no buffering with weaker feedback. **(B)** Slow buffering with stronger feedback reduces the adaptation error. In simulations the model parameters are $\theta_1 = 1,5$, $\theta_2 = 1$, $\gamma_p = 1$, $\eta = 100$, $\gamma_c = 0.05$, $B_1 = 0,5$, and $k = 1$ changes to $k = 0.7$ at $t = 100$.

thetic feedback and the addition of a protein buffer is:

$$\begin{aligned}
\dot{n} &= \alpha_n n(1-n) - \delta_n b_i n - \frac{\alpha_n n p}{p+\gamma_p} \\
\dot{b}_i &= \alpha_b n - \delta_b p b_i \\
\dot{p} &= k z_2 - \beta_p p - I r_p p + r_w w \\
\dot{b}_e &= V \delta_b p b_i n \\
\dot{z}_1 &= \mu - \eta z_1 z_2 \\
\dot{z}_2 &= \theta b_i - \eta z_1 z_2 \\
\dot{w} &= I r_p z_1 - r_w w
\end{aligned}$$

where n is the normalized cell density, which is assumed to follow logistic growth with additional death rates due to toxicity of intracellular biofuel concentration b_i and efflux protein pump p. The variables z_1 and z_2 are the controller species, while the production of the protein pump p is assumed to be proportional to controller species z_2. The variable w is the buffering species which buffers z_1 through a reversible reaction via chemical species I that inhibits z_1 sequestering when bound to z_1. The variable b_e is the extracellular concentration of biofuel.

Buffering of z_1 can be seen to stabilise the process in the simulations of the model (see Figure 6A). These simulations show that the oscillations, which occur when η is large, quickly settle to the steady state when buffering is introduced. This stabilising effect resembles impact of buffering in Topology 1 in Section III. It also shows the stabilising effect for models that are destabilised by strengthening the antithetic binding mechanism via increased η. This example thus illustrates that the stabilising effect of buffering also occurs in more complex systems than those considered in the previous section.

B. Model for growth control

For the synthetic growth control case study, we use an existing model of the synthetic growth control circuit, which includes the new addition of buffering[27] (see Figure 6). The variable N represents the population size and is assumed to follow logistic growth, with an additional death rate due to toxicity that is proportional to the concentration of $CcdB$ per cell. $Ccdb$ is a protein that is toxic to the cell. $mRNA$ is messenger RNA while $asRNA$ is a short antisense RNA that has a complementary sequence to the mRNA, which enables sequestration between the two. $mRNA$ and $asRNA$ form the antithetic integral controller. The transcription of mRNA is induced by a quorum-sensing ligand. The term G_a represents the gain between N and mRNA induction resulting from the quorum-sensing molecule AHL. W represents a buffer of Ccdb, which consists of an inactivated form of Ccdb that can reversibly bind to an inhibitor molecule I. The adapted model of the genetic circuit with the new addition of a protein buffer is

$$\begin{aligned}
\frac{d}{dt}[CcdB] &= k_p[mRNA] - (\gamma_p + b_C I)[CcdB] + b_w[W] \\
\frac{d}{dt}[mRNA] &= k_R G_a N - (\eta[asRNA] - \gamma_R)\,[mRNA] \\
\frac{d}{dt}[asRNA] &= \mu - \eta[asRNA][mRNA] - \gamma_R[asRNA] \\
\frac{d}{dt}N &= rN\left(1 - \frac{N}{N_m}\right) - \tau[CcdB]N \\
\frac{d}{dt}[W] &= b_C I[CcdB] - b_w[W] - \gamma_w[W]
\end{aligned}$$

where $[\cdot]$ represents intracellular concentrations for each species and the last line indicating the rate of change of W is new to the model.

The buffering of $CcdB$ as shown above is equivalent to x_1 buffering in the model (6) and Figure 2, as N is the output and equivalent to x_2. Buffering at x_1 provides a similar benefit as buffering at x_2 and so can also enable near-perfect adaptation, where we omitted these results in the previous section for brevity (see SI6).

Buffering of $CcdB$ in conjuction with increased feedback gain can be shown to reduce steady state error in the simulations in Figure 6. Increased feedback gain is implemented in these simulations by increasing the translation rate of $CcdB$.

VI. DISCUSSION

Perfect adaptation has been subject of intense study in the synthetic biology community. Although perfectly adapting systems are ubiquituous in nature, their implementation has proven particularly elusive. The antithetic control motif, first discovered by Briat et al[4] and

bioRxiv preprint doi: https://doi.org/10.1101/2021.04.18.440372; this version posted April 19, 2021. The copyright holder for this preprint (which was not certified by peer review) is the author/funder, who has granted bioRxiv a license to display the preprint in perpetuity. It is made available under aCC-BY-NC-ND 4.0 International license.

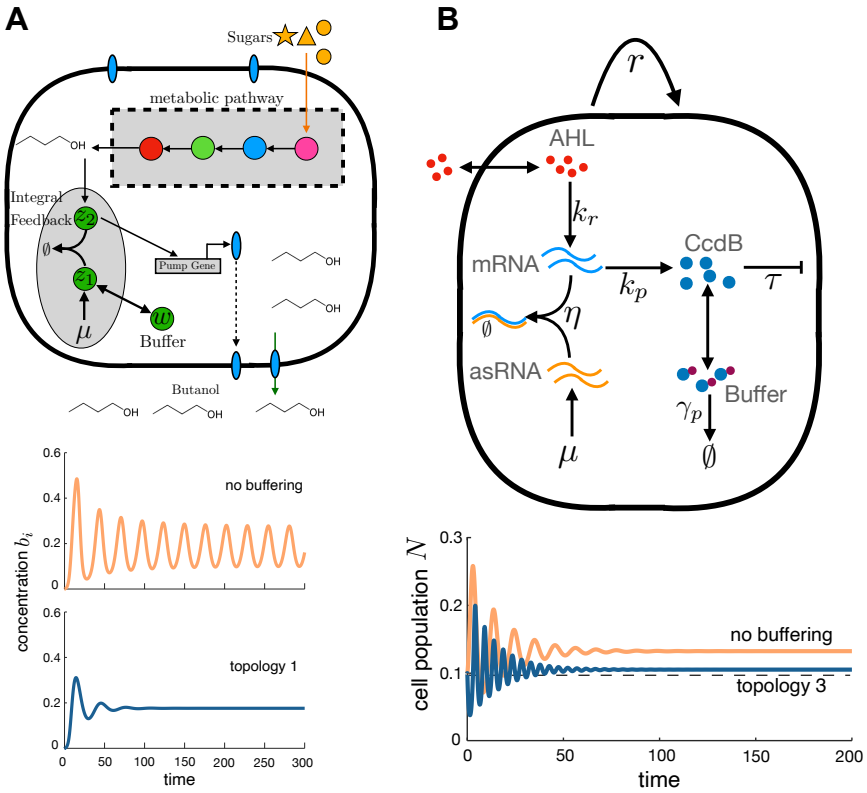

FIG. 6. Case studies of molecular buffering coupled with antithetic control. **(A)** Biofuel production system adapted from[6] to include buffering of species z_1. Simulations show the stabilising effect of buffering. Model parameters for simulations are $\alpha_n = 0.66$, $\delta_n = 0.5$, $\gamma_p = 0.14$, $\alpha_b = 0.1$, $\delta_b = 0.5$, $\beta_p = 0.66$, $V = 1$, $\eta = 5$, $\mu = 0.1762$, $\theta = 1$ $k = 0.5$, $r_p = 0$, $r_w = 0$, $\gamma_w = 0$, $I = 1$. **(B)** Synthetic growth control circuit[27] adapted to include buffering of CcdB. Simulations show the ability of buffering to decrease the steady state error via stronger feedback without oscillations. Model parameters for simulations without buffering are $k_p = 20$, $\gamma_p = 3$, $r = 1$, $\tau = 4 \times 10^{-3}$, $k_R = 10^{-1}$, $G = 10^{-6}$, $\eta = 20$, $\gamma_r = 0.1$, $\mu = 10$, $b_c = 0$, $b_w = 0$, $N_m = 10^9$, $\gamma_w = 0$. The buffered circuit has parameters $b_c = 300$, $b_w = 100$, $\gamma_w = 30$, $k_p = 3000$.

implemented by Aoki et al[1], provides a new molecular mechanism to build perfect adaptation into a wide range of synthetic gene circuits. A number of works have sought to find alternative circuits that provide adaptation properties similar to antithetic control. For example, several authors have shown that ultrasensitive feedback can display some of the features of perfect adaptation[25,28], and the idea was recently extended in great detail for synthetic gene circuits[30]. Other works have sought to devise molecular implementations of Proportional-Integral-Derivative control[9], as this is a widely adopted strategy for perfect adaptation in engineered control systems.

Here we have addressed caveats of the original antithetic control system with an extended architecture that has improved stability properties. The proposed circuit combines an antithetic motif with a molecular buffering mechanism. Molecular buffering is widely conserved in natural systems, and common examples include the ATP buffering by creatine phosphate, pH buffering and calcium buffering. In all these examples, a molecular buffer sequesters a target molecule into an inactive form, resulting in a system with improved ability to mitigate fast perturbations. In the case of antithetic control, the addition of buffering results in the stabilisation of unwanted oscillations and, moreover, provides near-perfect adaptation even in rapid growth conditions where the performance of antithetic control is known to be particularly poor.

After detailed examination of mathematical models for various circuit architectures (Fig. 2), we found two candidate systems with improved stability properties, either by buffering species of the antithetic motif itself, or by buffering and degrading a target species to be controlled. The first circuit, called topology 1 in Fig. 2, provides stability over a large range of parameters values than classic antithetic control and can generally stabilise the oscillations produced by antithetic control. Moreover, topology 1 requires buffering of a molecular species of the antithetic motif itself, and therefore it provides a promising strategy to stabilise variables that

bioRxiv preprint doi: https://doi.org/10.1101/2021.04.18.440372; this version posted April 19, 2021. The copyright holder for this preprint (which was not certified by peer review) is the author/funder, who has granted bioRxiv a license to display the preprint in perpetuity. It is made available under aCC-BY-NC-ND 4.0 International license.

are not easily buffered directly, such as population size or metabolite species as illustrated by the example in Fig 6A.

The second circuit, termed topology 3 in Fig. 2, requires buffering the molecular output of the process to be controlled. We found that, although in principle this topology can have a destabilising effect, when coupled with buffer degradation it provides an effective way to mitigate oscillations in fast growth regimes (Fig. 3). Interestingly, there is a similar effect when applied to intermediate species instead of the output species in the controlled process, such as x_1 in the original circuit shown in Fig. 2 or CcdB in the growth control case study in Fig. 6. Buffering an intermediate species also provides an alternative location when the output is not easily buffered. A drawback of topology 3 is that degradation of the buffer may require the implementation of additional molecular mechanisms. If the degradation mechanism requires expression of heterologous proteins, this can increase the genetic burden on the host cell and impair its physiology[8,26].

The effect of buffering on perfect adaptation is strikingly similar to a strategy employed in industrial process control, where buffer tanks are employed to regulate and smooth out the impact of disturbances[13]. In our case, the specific implementation of the molecular buffers is a subject of future study, as this will largely depend on the type of biomolecular process to be controlled. For example, buffers for gene expression may require gene products to be sequestered, which can be achieved through several mechanisms such as reversible protein-protein binding[24], phosphorylation[19] , small molecule inhibitors[11], or DNA decoy sites[34]. In metabolism and signalling systems, ubiquitous examples are the interconversion between a target species and a buffer (e. g. reversible catalysis between ATP and creatine phosphate[17,32]) or sequestering by dedicated proteins (e. g. Ca^{2+} or H^{+} ions[17,21,32]).

Our main goal in this paper was to show that molecular sequestration can improve perfect adaptation in the antithetic control motif. Since buffering is known to stabilise a much wider range of molecular networks[16], it also has the potential to improve other circuits implementing perfect adaptation, e. g. those that rely on ultrasensitive behaviour[30]. Another promising line of inquiry is investigating production feedback mechanisms with similar kinetic effects to degradation[16], which may enable topology 3 type buffers to stabilise the systems without an increase in burden. Further, the effect of nonlinear buffering reactions also requires investigation as these can produce an effective increase of the buffer equilibrium ratio without increasing the concentration of the buffer itself[18]. For simplicity, we have focused exclusively on deterministic dynamics, but the analysis of stochastic effects emerging from the interplay between molecular buffering and antithetic control are particularly attractive, as it is known that buffering does not amplify stochastic fluctuations[17] yet some phenomena are known to emerge only in the presence of molecular noise[4,31,33].

As synthetic gene circuits grow in size and complexity, there is a growing need for mechanisms that can enhance their robustness in a range of operational conditions. In the longer term, this will require the availability of a catalogue of gene circuits that can produce perfect adaptation in response to perturbations. In this work we have presented one such architecture, and thus laid theoretical groundwork for the discovery of new biomolecular systems with improved functionality.

METHODS

All mathematical models are based on systems of ordinary differential equations. The stability conditions in Eqs. (7), (8), (13) and (17) were obtained using frequency domain transformations (Laplace and Fourier) of the linearised models, along with detailed examination of the magnitude and phase equations of the resulting characteristic polynomials for the closed-loop systems[27]. Simulations were carried out using standard ODE solvers in MATLAB. All calculations and model descriptions can be found in the Supplementary Material.

AUTHOR CONTRIBUTIONS

Conceptualization, E.J.H.; Methodology, E.J.H.; Formal Analysis: E.J.H., and D.A.O.; Investigation, E.J.H., and D.A.O.; Writing - Original Draft, E.J.H. ; Writing - Review & Editing, E.J.H., and D.A.O. ; Funding Acquisition, E.J.H.; Supervision, E.J.H., and D.A.O.

ACKNOWLEDGEMENTS

The authors would like to thank Morgan Kelly for her assistance. EJH was would like to thank the contribution of Judith and David Coffey.

The authors declare that there are no competing interests.

REFERENCES

[1]S.K. Aoki, G. Lillacci ans A. Gupta, A. Baumschlager, D. Schweingruber, and M. Khammash. A universal biomolecular integral feedback controller for robust perfect adaptation. *Nature*, 570:533–537, 2019.

[2]K. J. Aström and R. M. Murray. *Feedback Systems*. Princeton University Press, 2008.

[3]N. Barkai and S. Leibler. Robustness in simple biochemical networks. *Nature*, 387:913–917, 1997.

bioRxiv preprint doi: https://doi.org/10.1101/2021.04.18.440372; this version posted April 19, 2021. The copyright holder for this preprint (which was not certified by peer review) is the author/funder, who has granted bioRxiv a license to display the preprint in perpetuity. It is made available under aCC-BY-NC-ND 4.0 International license.

[4]C. Briat, A. Gupta, and M. Khammash. Antithetic integral feedback ensures robust perfect adaptation in noisy biomolecular networks. *Cell Syst.*, 2(1):15–26, 2016.

[5]C. Briat, A. Gupta, and M. Khammash. Antithetic proportional-integral feedback for reduced variance and improved control performance of stochastic reaction networks. *Royal Society Interface*, 15, 2018.

[6]C. Briat and M. Khammash. Perfect adaptation and optimal equilibrium productivity in a simple microbial biofuel metabolic pathway using dynamic integral control. *ACS Synthetic Biology*, 7(2):419–431, 2018.

[7]D. E. Cameron, C.J. Bashor, and J. J. Collins. A brief history of synthetic biology. *Nat. Rev. Microbiol.*, 12(5):381–390, 2014.

[8]F. Ceroni, R. Algar, G. B. Stan, and T. Ellis. Quantifying cellular capacity identifies gene expression designs with reduced burden. *Nature Methods*, 12(5):415–418, apr 2015.

[9]M. Chevalier, M. Gomez-Schiavon, A.H. Ng, and H. El-Samad. Design and analysis of a proportional-integral- derivative controller with biological molecules. *Cell Systems*, 9:338–353, 2019.

[10]V. Chubukov, A. Mukhopadhyay, C.J. Petzold, J.D. Keasling, and H.G. Martin. Synthetic and systems biology for microbial production of commodity chemicals. *npj systems biology and applications*, 2(16009), 2016.

[11]C. Denison and T. Kodadek. Small-molecule-based strategies for controlling gene expression. *Chemistry Biology*, 5:129–145, 1998.

[12]M. J. Dunlop, J.D. Keasling, and A. Mukhopadhyay. A model for improving microbial biofuel production usinga synthetic feedback loop. *Syst Synth Biol*, 4:95=104, 2010.

[13]A. Faanes and S. Skogestad. Buffer tank design for acceptable control performance. *Ind. Eng. Chem. Res.*, 42(10):2198–2208, 2003.

[14]T. Friedlander and N. Brenner. Adaptive response by state-dependent inactivation. *Proc. Natl. Acad. Sci.*, 106(52):22558–22563, 2009.

[15]A. Gupta and M. Khammash. An antithetic integral rein controller for bio-molecular networks. *IEEE 58th Conference on Decision and Control (CDC), Nice, France,*, pages 2808–2813, 2019.

[16]E.J. Hancock and J.Ang. Frequency domain properties and fundamental limits of buffer–feedback regulation in biochemical systems. *Automatica*, 103:330–336, 2019.

[17]E.J. Hancock, J.Ang, A.Papachristodoulou, and G-B.Stan. The interplay between feedback and buffering in cellular homeostasis. *Cell Systems*, 5(5):498–508, 2017.

[18]E.J. Hancock, J.R. Krycer, and J. Ang. Metabolic buffer analysis reveals the simultaneous, independent control of atp and adenylate energy ratios. *Royal Society Interface*, in press, 2021.

[19]H. Harada, B. Becknell, M. Wilm, M. Mann, L.J. Huang, S.S. Taylor, J.D. Scott, and S.J. Korsmeyer. Phosphorylation and inactivation of bad by mitochondria-anchored protein kinase a. *Mol Cell*, 3(4):413–22, 1999.

[20]J.E. Ferrell Jr. Perfect and near-perfect adaptation in cell signaling. *Cell Systems*, 2:62–67, 2016.

[21]J. Keener and J. Sneyd. *Mathematical Physiology*. Springer-Verlag, 1998.

[22]D. Liu, A.A. Mannan, Y. Han, D.A. Oyarzún, and F. Zhang. Dynamic metabolic control: towards precision engineering of metabolism. *J Ind Microbiol Biotechnology*, 45(7):535–543, 2018.

[23]W. Ma, A. Trusina, H. El-Samad, W.A. Lim, , and C. Tang. Defining network topologies that can achieve biochemical adaptation. *Cell*, 138(4):760–73, 2009.

[24]J. De Melo, L. He, and D. Tang. The protein-protein interaction-mediated inactivation of pten. *Curr Mol Med*, 14(1):22–33, 2014.

[25]F. Montefusco, E.O. Akman, S.O. Soyer, and D. G. Bates. Ultrasensitive negative feedback control: A natural approach for the design of synthetic controllers. *PLOS One*, 11(8), 2016.

[26]E. M. Nikolados, A. Y. Weiße, F. Ceroni, and D. A. Oyarzún. Growth Defects and Loss-of-Function in Synthetic Gene Circuits. *ACS Synthetic Biology*, 8(6):1231–1240, 2019.

[27]N. Olsman, A-A. Baetica, F. Xiao, Y.P. Leong, R.M. Murray, and J.C. Doyle. Hard limits and performance tradeoffs in a class of antithetic integral feedback networks. *Cell Systems*, 9, 2019.

[28]D. A. Oyarzún and G.-B. Stan. Synthetic gene circuits for metabolic control: design trade-offs and constraints. *Journal of the Royal Society, Interface / the Royal Society*, 10(78), oct 2013.

[29]Y. Qian and D. Del Vecchio. Realizing 'integral control' in living cells: how to overcome leaky integration due to dilution? *Royal Society Interface*, 15, 2018.

[30]C.C. Samaniego and E. Franco. Ultrasensitive molecular controllers for quasi-integral feedback. *Cell Systems*, In Press, 2021.

[31]M. Samoilov, S. Plyasunov, and A. P. Arkin. Stochastic amplification and signaling in enzymatic futile cycles through noise-induced bistability with oscillations. *Proceedings of the National Academy of Sciences of the United States of America*, 102(7):2310–5, feb 2005.

[32]L. Sherwood. *Human Physiology: From Cells to Systems*. Brooks Cole, 2013.

[33]M. K. Tonn, P. Thomas, M. Barahona, and D. A. Oyarzún. Stochastic modelling reveals mechanisms of metabolic heterogeneity. *Communications Biology*, 2(1):108, dec 2019.

[34]T. Wang, N. Tague, S.A. Whelan, and M.J. Dunlop. Programmable gene regulation for metabolic engineering using decoy transcription factor binding sites. *Nucleic Acids Research*, 49(2):1163–1172, 2021.

[35]M. Wehrs, D. Tanjore, T. Eng, J. Lievense, T.R. Pray, and A. Mukhopadhyay. Engineering robust production microbes for large-scale cultivation. *Trends in Microbiology*, 27(6), 2019.

bioRxiv preprint doi: https://doi.org/10.1101/2021.04.18.440372; this version posted April 19, 2021. The copyright holder for this preprint (which was not certified by peer review) is the author/funder, who has granted bioRxiv a license to display the preprint in perpetuity. It is made available under aCC-BY-NC-ND 4.0 International license.

SUPPLEMENTARY MATERIAL

Stabilisation of Antithetic Control via Molecular Buffering

Edward J. Hancock [1,2], Diego A. Oyarzún[3,4]

[1] School of Mathematics and Statistics, The University of Sydney, NSW, 2006, Australia
[2] Charles Perkins Centre, The University of Sydney, NSW, 2006, Australia
[3] School of Biological Sciences, University of Edinburgh, UK
[4] School of Informatics, University of Edinburgh, UK

SI1. BUFFERING

In this section, we provide a background on buffering, including methods for analysing models with buffering. We start with the simple model in (3) of a single regulated species that is being buffered, such that

$$\begin{aligned} \dot{x} &= \underbrace{p(x)}_{\substack{\text{production}\\ \text{with feedback}}} - \underbrace{\gamma_x x}_{\text{removal}} + \underbrace{g_w(w) - g_x(x)}_{\text{buffering}} \\ \dot{w} &= \underbrace{g_x(x) - g_w(w)}_{\text{buffering}} - \underbrace{\gamma_w w}_{\text{removal}} \end{aligned} \tag{S1}$$

where x is the output species being regulated, w is the buffering species, p is the production rate of x, γ_x is the removal kinetic rate of x, g_w is the forward buffering reaction rate and g_x is the reverse buffering reaction rate. Incorporation of feedback is represented by the x dependence of production. The nominal steady state ($d = 0$) occurs when production matches degradation ($p(\bar{x}) = \gamma_x \bar{x} + \gamma_w \bar{w}$) and the buffer is at steady state ($g_w(\bar{w}) = g_x(\bar{x}) + \gamma_w \bar{w}$).
To analyse (S1), we reduce the two state model to one state by assuming that the buffering reactions rapidly reach equilibrium. To carry this out, we first linearise (S1), which results in

$$\begin{aligned} \Delta\dot{x} &= \underbrace{-h\Delta x}_{\text{feedback}} - \underbrace{\gamma_x \Delta x}_{\text{removal}} + \underbrace{b_w \Delta w - b_x \Delta x}_{\text{buffering}} \\ \Delta\dot{w} &= \underbrace{-b_w \Delta w + b_x \Delta x}_{\text{buffering}} - \underbrace{\gamma_w \Delta w}_{\text{removal}} \end{aligned}$$

where $h = -\frac{\partial p}{\partial x}$ is the linearised feedback gain, and $b_w = \frac{\partial g_w}{\partial w}$ and $b_x = \frac{\partial g_x}{\partial x}$ are the linearised kinetic rates for the forward and reverse buffering reaction.
If we assume that the buffer rapidly reaches equilibrium then w is at quasi-steady state and so $\Delta\dot{w} = -b_w \Delta w + (b_x + \gamma_w)\Delta x = 0$. This steady state results in

$$B = \frac{\Delta w}{\Delta x} = \frac{b_x}{b_w + \gamma_w}.$$

We set the slow variable as $\Delta x_T = \Delta w + \Delta x$ where $\Delta\dot{x}_T = -(h + \gamma_x)\Delta x - \gamma_w \Delta w$. Using the definition of B above, we have $\Delta x_T = (1 + B)\Delta x$. Thus $\Delta\dot{x}_T = (1 + B)\Delta\dot{x}$ and so

$$\boxed{(1 + B)\Delta\dot{x} = -h\Delta x - (\gamma_p + B\gamma_w)\Delta x}$$

which is a reduced one state model, where the second state can be determined from $\Delta w = B\Delta x$.
In technology, integral feedback is often paired with proportional and derivative feedback (PID control)[2]. In biology, rapid buffering without degradation is equivalent to negative derivative feedback and rapid buffering with degradation is equivalent to PD feedback with degradation. These equivalences can be observed in[17]

$$\Delta\dot{x} = \underbrace{-B\Delta\dot{x} - \gamma_w B\Delta x}_{\substack{\text{proportional +}\\ \text{derivative}\\ \text{feedback}}} - \underbrace{h\Delta x}_{\substack{\text{proportional}\\ \text{feedback}}} - \gamma_p \Delta x$$

bioRxiv preprint doi: https://doi.org/10.1101/2021.04.18.440372; this version posted April 19, 2021. The copyright holder for this preprint (which was not certified by peer review) is the author/funder, who has granted bioRxiv a license to display the preprint in perpetuity. It is made available under aCC-BY-NC-ND 4.0 International license.

where the buffer equilibrium ratio B corresponds to the derivative feedback 'gain'.
To study the effect of buffering on stability, we can also modify the model in (S1) to include a delay of the production feedback term

$$\begin{aligned} \dot{x} &= \underbrace{p(x(t-\tau))}_{\substack{\text{production}\\ \text{with feedback}}} - \underbrace{\gamma_x x}_{\text{removal}} + \underbrace{g_w(w) - g_x(x)}_{\text{buffering}} \\ \dot{w} &= \underbrace{g_x(x) - g_w(w)}_{\text{buffering}} - \underbrace{\gamma_w w}_{\text{removal}} \end{aligned} \tag{S2}$$

where $p(x(t-\tau))$ represents the production feedback with a delay of time τ. The reduced model is

$$\boxed{(1+B)\Delta\dot{x} = -h\Delta x_\tau - (\gamma_p + B\gamma_w)\Delta x}$$

where $\Delta x_\tau = \Delta x(t-\tau)$.
It can be observed in Figure S1 that buffering can stabilise the oscillations that result from feedback delay.

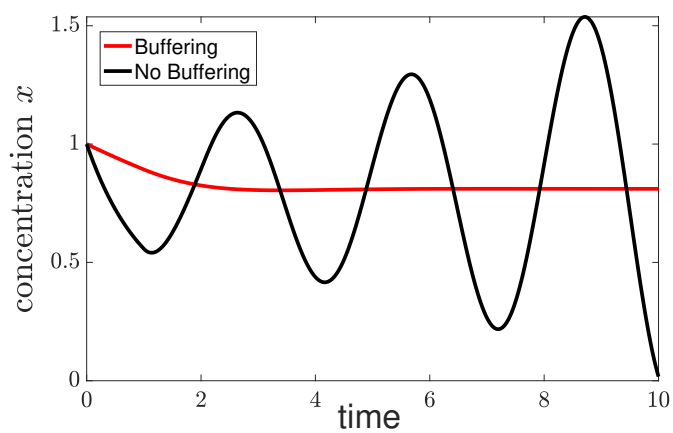

FIG. S1. The parameters are $B_x = 0$ and 5, $\tau = 1$ (delay), $\gamma_p = 1$, $\gamma_w = 0$ and $h = 2.7$.

SI2. BUFFERING CAN STABILISE ANTITHETIC INTEGRAL FEEDBACK: ALL SPECIES

In this section, we analyse the stabilising effect of buffering (without degradation) on antithetic integral feedback. We base our studies on a simple model involving the antithetic integral feedback (without buffering)[27]. Consider

$$\begin{aligned} \dot{x}_1 &= \theta_1 z_1 - \gamma_p x_1 \\ \dot{x}_2 &= k x_1 - \gamma_p x_2 \\ \dot{z}_1 &= \mu - \eta z_1 z_2 \\ \dot{z}_2 &= \theta_2 x_2 - \eta z_1 z_2 \end{aligned} \tag{S3}$$

where x_2 is the output concentration being controlled, x_1 is another concentration in the process being controlled, and z_1 and z_2 represent the molecular species involved in the perfect adaptation mechanism.
We next introduce buffering to (S3). We show how the model reduction method described in SI1 can be used to simplify the model for one case. We then use the same method for all buffers.
As a first case, we introduce buffering at the controlled variable x_2 and simplify the model by assuming that the

bioRxiv preprint doi: https://doi.org/10.1101/2021.04.18.440372; this version posted April 19, 2021. The copyright holder for this preprint (which was not certified by peer review) is the author/funder, who has granted bioRxiv a license to display the preprint in perpetuity. It is made available under aCC-BY-NC-ND 4.0 International license.

buffering reactions rapidly reach equilibrium. With buffering at x_2, we have

$$\begin{aligned}\dot{x}_1 &= \theta_1 z_1 - \gamma_p x_1\\ \dot{x}_2 &= k x_1 - \gamma_p x - \gamma_p x_2 - b_x x + b_w w\\ \dot{z}_1 &= \mu - \eta z_1 z_2\\ \dot{z}_2 &= \theta_2 x_2 - \eta z_1 z_2\\ \dot{w}_x &= b_x x_2 - b_w w_x\end{aligned} \tag{S4}$$

where w_x is the buffering species at x_2 and b_x, b_w are the kinetic rate constants for the buffering reactions. Although the buffering equilibrium ratio is defined in terms of the linearised model and deviations from steady state, we can use the same notation here for the nonlinear model as the buffering reactions are linear. If the buffering reaction is at equilibrium then

$$b_x x_2 = b_w w_x.$$

If we assume that the buffer rapidly reaches equilibrium then w is at quasi-steady state and so

$$w_x = B_x x_2 \quad B_x = \frac{b_x}{b_w}.$$

We note that although the buffer equilibrium ratio is defined in (5) in terms deviations from steady state, we can use the buffer equilibrium ratios in the nonlinear model as the reaction rates are linear.
We set $x_T = w_x + x$ as the slow variable and so $x_T = (1 + B_x)x_2$. Thus $\dot{x}_T = (1 + B_x)\dot{x}_2$ and so

$$(1 + B_x)\dot{x}_2 = k x_1 - \gamma_p x_2.$$

If we include buffering on z_1, z_2, x_2 and apply a similar model reduction by assuming rapid buffering, then we have

$$\begin{aligned}\dot{x}_1 &= \theta_1 z_1 - \gamma_p x_1\\ (1 + B_x)\dot{x}_2 &= k x_1 - \gamma_p x_2\\ (1 + B_1)\dot{z}_1 &= \mu - \eta z_1 z_2\\ (1 + B_2)\dot{z}_2 &= \theta_2 x_2 - \eta z_1 z_2\end{aligned} \tag{S5}$$

where B_1, B_2 are the buffer equilibrium ratios of the buffers at z_1 and z_2 respectively.

A. Steady State

We first determine the steady states of the system, which is useful both for determining perfect adaptation and as a prerequisite for stability analysis. Using

$$(1 + B_1)\dot{z}_1 - (1 + B_2)\dot{z}_2 = \mu - \theta_2 x_2 = 0$$

we can see that the steady state for the output is

$$\bar{x}_2 = \frac{\mu}{\theta_2}.$$

The correspondence of this steady state with perfect adaptation is discussed further in Section II A and III. The species x_1, z_1 and z_2 have the corresponding steady states

$$\bar{x}_1 = \frac{\mu\gamma_p}{\theta_2 k}, \quad \bar{z}_1 = \frac{\gamma_p^2 \mu}{\theta_1\theta_2 k}, \quad \bar{z}_2 = \frac{\theta_1\theta_2 k}{\eta\gamma_p^2}.$$

bioRxiv preprint doi: https://doi.org/10.1101/2021.04.18.440372; this version posted April 19, 2021. The copyright holder for this preprint (which was not certified by peer review) is the author/funder, who has granted bioRxiv a license to display the preprint in perpetuity. It is made available under aCC-BY-NC-ND 4.0 International license.

B. Stability

We next determine the effect of buffering on the stability of the model. We follow the methodology used by Olsman and colleagues[27] to study the stability of antithetic integral feedback with the addition of buffering. Linearising the system (S5) about the steady states, we have

$$\begin{aligned}
\Delta\dot{x}_1 &= \theta_1\Delta z_1 - \gamma_p\Delta x_1 \\
(1+B_x)\Delta\dot{x}_2 &= k\Delta x_1 - \gamma_p\Delta x_2 \\
(1+B_1)\Delta\dot{z}_1 &= -\alpha\Delta z_1 - \frac{\beta}{\alpha}\Delta z_2 \\
(1+B_2)\Delta\dot{z}_2 &= \theta_2\Delta x_2 - \alpha\Delta z_1 - \frac{\beta}{\alpha}\Delta z_2
\end{aligned} \tag{S6}$$

where $\Delta z_1 = z_1 - \bar{z}_1$, $\Delta z_2 = z_2 - \bar{z}_2$, $\Delta x_1 = x_1 - \bar{x}_1$, $\Delta x_2 = x_2 - \bar{x}_2$ are the deviations from steady state and

$$\alpha = \frac{\theta_1\theta_2 k}{\gamma_p^2}, \quad \beta = \eta\mu.$$

Taking the Laplace transform of (S6), we have

$$\begin{aligned}
(s+\gamma_p)X_1 &= \theta_1 Z_1 \\
((1+B_x)s+\gamma_p)X_2 &= kX_1 \\
((1+B_1)s+\alpha)Z_1 &= -\frac{\beta}{\alpha}Z_2 \\
\left((1+B_2)s+\frac{\beta}{\alpha}\right)Z_2 &= \theta_2 X_2 - \alpha Z_1
\end{aligned} \tag{S7}$$

where $Z_1 = \mathcal{L}\{\Delta z_1\}$, $Z_2 = \mathcal{L}\{\Delta z_2\}$, $X_1 = \mathcal{L}\{\Delta x_1\}$, $X_2 = \mathcal{L}\{\Delta x_2\}$ are the Laplace transforms of the time-domain concentration deviations. Substituting, we have

$$\begin{aligned}
(s+\gamma_p)((1+B_x)s+\gamma_p)X_2 &= \theta_1 k Z_1 \\
\left((1+B_2)s+\frac{\beta}{\alpha}\right)((1+B_1)s+\alpha)Z_1 &= -\frac{\beta}{\alpha}(\theta_2 X_2 - \alpha Z_1).
\end{aligned} \tag{S8}$$

Simplifying, we have

$$(1+B_1)(1+B_2)\left(s^2 + \left(\frac{\beta}{\alpha(1+B_2)} + \frac{\alpha}{1+B_1}\right)s\right)Z_1 = -\frac{\beta}{\alpha}\theta_2 X_2.$$

Substituting from (S8), we have

$$\left[(1+B_1)(1+B_2)s((1+B_x)s+\gamma_p)(s+\gamma_p)\left(s+\frac{\beta}{\alpha(1+B_2)}+\frac{\alpha}{1+B_1}\right)+\frac{\beta}{\alpha}\theta_1\theta_2 k\right]X_2 = 0.$$

The characteristic equation used to analyse stability is thus

$$s((1+B_x)s+\gamma_p)(s+\gamma_p)\left(s+\frac{\beta}{\alpha(1+B_2)}+\frac{\alpha}{1+B_1}\right)+\frac{\beta\gamma_p^2}{(1+B_1)(1+B_2)} = 0. \tag{S9}$$

1. Characterisation of roots

Following the methodology used by Olsman and colleagues[27], we first characterise the roots of (S9). If we substitute $s = \gamma_p\sigma$ then

$$\sigma(1+\sigma)\left(1+(1+B_x)\sigma\right)\left(\sigma+\frac{\beta}{\gamma_p\alpha(1+B_2)}+\frac{\alpha}{\gamma_p(1+B_1)}\right) = -\frac{\beta}{\gamma_p^2(1+B_1)(1+B_2)}. \tag{S10}$$

bioRxiv preprint doi: https://doi.org/10.1101/2021.04.18.440372; this version posted April 19, 2021. The copyright holder for this preprint (which was not certified by peer review) is the author/funder, who has granted bioRxiv a license to display the preprint in perpetuity. It is made available under aCC-BY-NC-ND 4.0 International license.

Taking the limit of strong binding for the sequestration process in antithetic integral feedback $\left(\beta \gg \max\left\{\alpha^2 \frac{(1+B_2)}{(1+B_1)}, \alpha\gamma_p(1+B_2)\right\}\right)$ then

$$\sigma(1+\sigma)\left(1+(1+B_x)\sigma\right)\left(1+\sigma\frac{\gamma_p\alpha(1+B_2)}{\beta}\right) = -\frac{\alpha}{\gamma_p(1+B_1)}.$$

It can be observed that there is a large, real root at $\sigma \approx -\frac{\beta}{\gamma_p\alpha(1+B_2)}$. We next examine the region $|\sigma| \ll \frac{\beta}{\gamma_p\alpha(1+B_2)}$, where we have

$$\sigma(1+\sigma)\left(1+(1+B_x)\sigma\right) = -\frac{\alpha}{\gamma_p(1+B_1)}.$$

The magnitude and phase constraints are

$$|\sigma||1+\sigma||1+(1+B_x)\sigma| = \frac{\alpha}{\gamma_p(1+B_1)}$$
$$\arg\sigma + \arg(1+\sigma) + \arg\left(1+(1+B_x)\sigma\right) = (1+2k)\pi.$$

If we assume that σ is real and positive, then the LHS of the phase constraint is

$$\arg\sigma + \arg(1+\sigma) + \arg\left(1+(1+B_x)\sigma\right) = 0$$

which contradicts. Thus unstable roots are not purely real.
If we assume that σ is real and $-1/(1+B_x) < \sigma < 0$ then the LHS of the phase constraint is

$$\arg\sigma + \arg(1+\sigma) + \arg\left(1+(1+B_x)\sigma\right) = \pi$$

and so it is possible to have stable real roots. If we set $f = |\sigma||1+\sigma||1+(1+B_x)\sigma|$ from the magnitude constraint, then there is a local maxim of f at

$$\sigma_{max} = \frac{-(2+B_x)+\sqrt{1+B_x+B_x^2}}{3(1+B_x)}.$$

Thus there are two stable real roots between $-1/(1+B_x) < \sigma < 0$ if

$$f(\sigma_{max}) > \frac{\alpha}{\gamma_p(1+B_1)}$$

as $f(\sigma_{max})$ is larger than the RHS of the magnitude constraint. There is a bifurcation at the boundary $f(\sigma_{max}) = \frac{\alpha}{\gamma_p(1+B_1)}$ resulting in a pair of complex conjugate roots if

$$f(\sigma_{max}) < \frac{\alpha}{\gamma_p(1+B_1)}.$$

For $-1 < \sigma < -1/(1+B_x)$ then

$$\arg\sigma + \arg(1+\sigma) + \arg\left(1+(1+B_x)\sigma\right) = 2\pi$$

which violates the phase constraints. For $\sigma < -1$ then

$$\arg\sigma + \arg(1+\sigma) + \arg\left(1+(1+B_x)\sigma\right) = 3\pi$$

which meets the phase constraints. Thus for the stability boundary with strong binding there is a negative real root and a complex pair of roots in the region $|\sigma| \ll \frac{\beta}{\gamma_p\alpha(1+B_2)}$, as well as one large negative root.

bioRxiv preprint doi: https://doi.org/10.1101/2021.04.18.440372; this version posted April 19, 2021. The copyright holder for this preprint (which was not certified by peer review) is the author/funder, who has granted bioRxiv a license to display the preprint in perpetuity. It is made available under aCC-BY-NC-ND 4.0 International license.

2. Stability Conditions

To determine the stability boundary, we next determine the conditions for which the complex roots are purely imaginary. Substituting $s = i\omega\gamma_p$, we have

$$\gamma_p^4 i\omega(1+i\omega)(1+(1+B_x)i\omega)\left(i\omega+\left(\frac{\beta}{\alpha\gamma_p(1+B_2)}+\frac{\alpha}{\gamma_p(1+B_1)}\right)\right) = -\frac{\beta\gamma_p^2}{(1+B_1)(1+B_2)}.$$

From these equations, the magnitude and phase constraint are

$$\begin{aligned}
&\omega(1+\omega^2)^{0.5}(1+(1+B_x)^2\omega^2)^{0.5}\left(\omega^2+\phi^2\right)^{0.5} = \frac{\beta}{\gamma_p^2(1+B_1)(1+B_2)}\\
&\tan^{-1}(\omega)+\tan^{-1}((1+B_x)\omega)+\tan^{-1}\left(\frac{\omega}{\phi}\right) = \frac{\pi}{2}+2k\pi\\
&\phi = \frac{\beta}{\alpha\gamma_p(1+B_2)}+\frac{\alpha}{\gamma_p(1+B_1)}
\end{aligned}$$

for some integer k. Using the strong binding assumption $\left(\beta \gg \max\left\{\alpha^2\frac{(1+B_2)}{(1+B_1)}, \alpha\gamma_p(1+B_2)\right\}\right)$ then from above $|\omega| \ll \frac{\beta(1+B_1)}{\gamma_p\alpha(1+B_2)}$ and so

$$\begin{aligned}
\omega(1+\omega^2)^{0.5}(1+(1+B_x)^2\omega^2)^{0.5} &= \frac{\alpha}{\gamma_p(1+B_1)}\\
\tan^{-1}(\omega)+\tan^{-1}((1+B_x)\omega) &= \frac{\pi}{2}+2k\pi.
\end{aligned}$$

Rewriting the phase constraint, we have

$$\tan^{-1}(\omega)-\frac{\pi}{4} = \frac{\pi}{4}-\tan^{-1}((1+B_x)\omega).$$

Applying $\tan(\cdot)$ and trigonometric identities to both sides, we have

$$\frac{\omega-1}{\omega+1} = \frac{1-(1+B_x)\omega}{1+(1+B_x)\omega}.$$

Solving, we have

$$\omega = \frac{1}{\sqrt{1+B_x}}.$$

Thus the stability boundary occurs at

$$\gamma_p = \frac{\alpha}{(1+B_1)}\frac{1+B_x}{2+B_x}.$$

From above, we know that all roots are real and stable if $\alpha/(\gamma_p(1+B_1))$ is sufficiently small, and so the stability condition is

$$\gamma_p > \frac{\alpha}{(1+B_1)}\frac{1+B_x}{2+B_x}$$

or

$$\boxed{\gamma_p^3 > \frac{\theta_1\theta_2 k}{(1+B_1)}\frac{1+B_x}{2+B_x}}.$$

Thus increasing B_1 improves stability and increasing B_2 has no effect on stability. Further, increasing B_x worsens stability, although this effect saturates as B_x increases.

bioRxiv preprint doi: https://doi.org/10.1101/2021.04.18.440372; this version posted April 19, 2021. The copyright holder for this preprint (which was not certified by peer review) is the author/funder, who has granted bioRxiv a license to display the preprint in perpetuity. It is made available under aCC-BY-NC-ND 4.0 International license.

SI3. BUFFERING CAN STABILISE ANTITHETIC INTEGRAL FEEDBACK: x_2 BUFFERING WITH DEGRADATION

In this section, we analyse the stabilising effect of buffering at the output species x_2 on antithetic integral feedback, where the buffering can be degraded. Consider the model (S4) with buffering at x_2 that is degraded

$$\begin{aligned}
\dot{x}_1 &= \theta_1 z_1 - \gamma_p x_1 \\
\dot{x}_2 &= k x_1 - \gamma_p x_2 - b_x x_2 + b_w w_x \\
\dot{w}_x &= b_x x_2 - b_w w_x - \gamma_x w_x \\
\dot{z}_1 &= \mu - \eta z_1 z_2 \\
\dot{z}_2 &= \theta_2 x_2 - \eta z_1 z_2
\end{aligned}$$

where w_x is the buffering species of x_2, and b_x, b_w are the kinetic rates for the buffering reactions. If we assume rapid buffering such that $w_x + x_2$ is the slow variable, $w_x = B_x x_2$ and $B_x = \frac{b_x}{b_w + \gamma_x}$, and use the methodology from SI1 and SI2 then we have the reduced model

$$\begin{aligned}
\dot{x}_1 &= \theta_1 z_1 - \gamma_p x_1 \\
(1 + B_x)\dot{x}_2 &= k x_1 - (\gamma_p + B_x \gamma_x) x_2 \\
\dot{z}_1 &= \mu - \eta z_1 z_2 \\
\dot{z}_2 &= \theta_2 x_2 - \eta z_1 z_2.
\end{aligned}$$

Steady State Analysis

We next analyse the steady state. We have

$$\dot{z}_1 - \dot{z}_2 = \mu - \theta_2 x_2$$

and so the steady state of the output is

$$x_2 = \frac{\mu}{\theta_2}.$$

We also have corresponding steady states

$$\begin{aligned}
x_1 &= \frac{\gamma_p}{k}\left(1 + B_x \frac{\gamma_x}{\gamma_p}\right)\frac{\mu}{\theta_2} \\
z_1 &= \frac{\gamma_p}{\theta_1} x_1 = \frac{\gamma_p^2 \mu}{\theta_1 k \theta_2}\left(1 + B_x \frac{\gamma_x}{\gamma_p}\right) = \frac{\mu}{\alpha}\left(1 + B_x \frac{\gamma_x}{\gamma_p}\right) \\
z_2 &= \frac{1}{\eta}\frac{\mu}{z_1} = \frac{\alpha}{\eta\left(1 + B_x \frac{\gamma_x}{\gamma_p}\right)}
\end{aligned}$$

where $\alpha = \frac{\theta_1 \theta_2 k}{\gamma_p^2}$.

Stability Analysis

We next analyse the stability of the system. If we linearise about the steady states, we have

$$\begin{aligned}
\Delta\dot{x}_1 &= \theta_1 \Delta z_1 - \gamma_p \Delta x_1 \\
(1 + B_x)\Delta\dot{x}_2 &= k \Delta x_1 - \gamma_p\left(1 + B_x \frac{\gamma_x}{\gamma_p}\right)\Delta x_2 \\
\Delta\dot{z}_1 &= -\eta \bar{z}_2 \Delta z_1 - \eta \bar{z}_1 \Delta z_2 \\
\Delta\dot{z}_2 &= \theta_2 \Delta x_2 - \eta \bar{z}_2 \Delta z_1 - \eta \bar{z}_1 \Delta z_2.
\end{aligned}$$

bioRxiv preprint doi: https://doi.org/10.1101/2021.04.18.440372; this version posted April 19, 2021. The copyright holder for this preprint (which was not certified by peer review) is the author/funder, who has granted bioRxiv a license to display the preprint in perpetuity. It is made available under aCC-BY-NC-ND 4.0 International license.

This system can be rewritten as

$$\begin{aligned}
\Delta\dot{x}_1 &= \theta_1 \Delta z_1 - \gamma_p \Delta x_1 \\
(1+B_x)\Delta\dot{x}_2 &= k\Delta x_1 - \gamma_p \left(1 + B_x \frac{\gamma_x}{\gamma_p}\right) \Delta x_2 \\
\Delta\dot{z}_1 &= -\frac{\alpha}{\left(1+B_x\frac{\gamma_x}{\gamma_p}\right)} \Delta z_1 - \frac{\beta\left(1+B_x\frac{\gamma_x}{\gamma_p}\right)}{\alpha} \Delta z_2 \\
\Delta\dot{z}_2 &= \theta_2 \Delta x_2 - \frac{\alpha}{\left(1+B_x\frac{\gamma_x}{\gamma_p}\right)} \Delta z_1 - \frac{\beta\left(1+B_x\frac{\gamma_x}{\gamma_p}\right)}{\alpha} \Delta z_2.
\end{aligned}$$

where $\alpha = \frac{\theta_1\theta_2 k}{\gamma_p^2}$ and $\beta = \eta\mu$. Taking the Laplace transforms, we have

$$\begin{aligned}
&(s+\gamma_p)X_1 = \theta_1 Z_1 \\
&(1+B_x)\left(s + \frac{\gamma_p + B_x\gamma_x}{1+B_x}\right) X_2 = kX_1 \\
&\left(s + \frac{\alpha}{\left(1+B_x\frac{\gamma_x}{\gamma_p}\right)}\right) Z_1 = -\frac{\beta\left(1+B_x\frac{\gamma_x}{\gamma_p}\right)}{\alpha} Z_2 \\
&\left(s + \frac{\beta\left(1+B_x\frac{\gamma_x}{\gamma_p}\right)}{\alpha}\right) Z_2 = \theta_2 X_2 - \frac{\alpha}{\left(1+B_x\frac{\gamma_x}{\gamma_p}\right)} Z_1
\end{aligned}$$

where $Z_1 = \mathcal{L}\{\Delta z_1\}$, $Z_2 = \mathcal{L}\{\Delta z_2\}$, $X_1 = \mathcal{L}\{\Delta x_1\}$, $X_2 = \mathcal{L}\{\Delta x_2\}$ are the Laplace transforms of the time-domain concentration deviations. Substituting, we have

$$\begin{aligned}
&(1+B_x)(s+\gamma_p)\left(s + \frac{\gamma_p + B_x\gamma_x}{1+B_x}\right) X_2 = \theta_1 k Z_1 \\
&\left(s + \frac{\alpha}{\left(1+B_x\frac{\gamma_x}{\gamma_p}\right)}\right)\left(s + \frac{\beta\left(1+B_x\frac{\gamma_x}{\gamma_p}\right)}{\alpha}\right) Z_1 \\
&= -\frac{\beta\left(1+B_x\frac{\gamma_x}{\gamma_p}\right)}{\alpha}\left(\theta_2 X_2 - \frac{\alpha}{\left(1+B_x\frac{\gamma_x}{\gamma_p}\right)} Z_1\right).
\end{aligned}$$

Rewriting and substituting, we have

$$\begin{aligned}
&(1+B_x)(s+\gamma_p)\left(s + \frac{\gamma_p + B_x\gamma_x}{1+B_x}\right) s \left(s + \frac{\alpha}{\left(1+B_x\frac{\gamma_x}{\gamma_p}\right)} + \frac{\beta\left(1+B_x\frac{\gamma_x}{\gamma_p}\right)}{\alpha}\right) X_2 \\
&= -\frac{\beta\left(1+B_x\frac{\gamma_x}{\gamma_p}\right)}{\alpha}\theta_1\theta_2 k X_2.
\end{aligned}$$

Simplifying and taking the limit of strong binding for the sequestration process in the antithetic integral feedback $\left(\beta \gg \frac{\alpha^2}{\left(1+B_x\frac{\gamma_x}{\gamma_p}\right)^2}, \frac{\alpha\gamma_p}{\left(1+B_x\frac{\gamma_x}{\gamma_p}\right)}\right)$ then

$$(1+B_x)(s+\gamma_p)\left(s + \frac{\gamma_p + B_x\gamma_x}{1+B_x}\right) s \left(s + \frac{\beta\left(1+B_x\frac{\gamma_x}{\gamma_p}\right)}{\alpha}\right) X_2 = -\frac{\beta\left(1+B_x\frac{\gamma_x}{\gamma_p}\right)}{\alpha}\theta_1\theta_2 k X_2.$$

bioRxiv preprint doi: https://doi.org/10.1101/2021.04.18.440372; this version posted April 19, 2021. The copyright holder for this preprint (which was not certified by peer review) is the author/funder, who has granted bioRxiv a license to display the preprint in perpetuity. It is made available under aCC-BY-NC-ND 4.0 International license.

Thus we have the characteristic equation

$$(1+B_x)(s+\gamma_p)\left(s+\frac{\gamma_p+B_x\gamma_x}{1+B_x}\right)s\left(s+\frac{\beta\left(1+B_x\frac{\gamma_x}{\gamma_p}\right)}{\alpha}\right)+\beta\gamma_p^2\left(1+B_x\frac{\gamma_x}{\gamma_p}\right)=0.$$

Substituting $s=\gamma_p\sigma$, we have

$$(1+B_x)(1+\sigma)\left(\sigma+\frac{1+B_x\frac{\gamma_x}{\gamma_p}}{1+B_x}\right)\sigma\left(\sigma+\frac{\beta\left(1+B_x\frac{\gamma_x}{\gamma_p}\right)}{\gamma_p\alpha}\right)=-\frac{\beta}{\gamma_p^2}\left(1+B_x\frac{\gamma_x}{\gamma_p}\right).$$

Using the same argument as that in SI2, for the stability boundary with strong binding there is a negative real and complex pair of roots in the region $|\sigma|\ll\frac{\beta\left(1+B_x\frac{\gamma_x}{\gamma_y}\right)}{\gamma_p\alpha}$, as well as one large negative root.
To determine the boundary of stability, we next determine the conditions for which the roots are purely imaginary. Substituting $s=i\omega\gamma_p$, we have

$$(1+B_x)(1+i\omega)\left(i\omega+\frac{1+B_x\frac{\gamma_x}{\gamma_p}}{1+B_x}\right)i\omega\left(i\omega+\frac{\beta\left(1+B_x\frac{\gamma_x}{\gamma_p}\right)}{\gamma_p\alpha}\right)=-\frac{\beta}{\gamma_p^2}\left(1+B_x\frac{\gamma_x}{\gamma_p}\right).$$

Taking the strong binding limit where $|i\omega|\ll\frac{\beta\left(1+B_x\frac{\gamma_x}{\gamma_y}\right)}{\gamma_p\alpha}$, we have

$$(1+i\omega)\left(i\omega+\frac{1+B_x\frac{\gamma_x}{\gamma_p}}{1+B_x}\right)i\omega=-\frac{\alpha}{\gamma_p(1+B_x)}.$$

The phase and magnitude constraints are

$$(1+\omega^2)^{0.5}\left(\omega^2+\left(\frac{1+B_x\frac{\gamma_x}{\gamma_p}}{1+B_x}\right)^2\right)^{0.5}\omega=\frac{\alpha}{\gamma_p(1+B_x)}$$
$$\tan^{-1}(\omega)+\tan^{-1}\left(\frac{1+B_x}{1+B_x\frac{\gamma_x}{\gamma_p}}\omega\right)=\frac{\pi}{2}+2k\pi$$

for some integer k. Solving the phase constraint, we have

$$\frac{\omega-1}{1+\omega}=\frac{1-C\omega}{1+C\omega}$$
$$C=\frac{1+B_x}{1+B_x\frac{\gamma_x}{\gamma_p}}.$$

For this constraint we require

$$C\omega^2=1$$

which reduces to

$$\omega^2=\frac{1+B_x\frac{\gamma_x}{\gamma_p}}{1+B_x}.$$

Substituting into the magnitude equation, we have

$$\frac{\alpha}{\gamma_p(1+B_x)}=(1+C)^{0.5}\left(C+C^{-2}\right)^{0.5}C^{-0.5}$$
$$=(1+C)C.$$

bioRxiv preprint doi: https://doi.org/10.1101/2021.04.18.440372; this version posted April 19, 2021. The copyright holder for this preprint (which was not certified by peer review) is the author/funder, who has granted bioRxiv a license to display the preprint in perpetuity. It is made available under aCC-BY-NC-ND 4.0 International license.

Rearranging, we have the stability condition

$$\boxed{\gamma_p^3 > \frac{\theta_1\theta_2 k}{2+\left(1+\frac{\gamma_x}{\gamma_p}\right)B_x}\frac{1+B_x}{1+\frac{\gamma_x}{\gamma_p}B_x}}.$$

We can differentiate the right hand side with respect to B_x to determine whether increasing B_x has a stabilising effect. If we set

$$f(B_x) = \frac{1+B_x}{\left(2+\left(1+\frac{\gamma_x}{\gamma_p}\right)B_x\right)\left(1+\frac{\gamma_x}{\gamma_p}B_x\right)}.$$

then

$$\frac{\partial f}{\partial B_x} = \frac{1-3\frac{\gamma_x}{\gamma_p}-2\frac{\gamma_x}{\gamma_p}\left(1+\frac{\gamma_x}{\gamma_p}\right)B_x-(1+\frac{\gamma_x}{\gamma_p})\frac{\gamma_x}{\gamma_p}B_x^2}{\left(2+\left(1+\frac{\gamma_x}{\gamma_p}\right)B_x\right)^2\left(1+\frac{\gamma_x}{\gamma_p}B_x\right)^2}.$$

Thus for small B_x then buffering stabilises antithetic integral feedback if $\gamma_x > \frac{1}{3}\gamma_p$. For large B_x then increasing B_x improves stability if $\gamma_x > 0$.

SI4. RAPID x_1 BUFFERING WITH DEGRADATION CAN STABILISE ANTITHETIC INTEGRAL FEEDBACK

In this section, we analyse the stabilising effect of buffering at the intermediate species x_1 on antithetic integral feedback, where the buffering can be degraded. This section uses identical methodology and obtains equivalent results to SI3.
Consider the model (S3) with buffering at x_1 that is degraded

$$\begin{aligned}
\dot{x}_1 &= \theta_1 z_1 - \gamma_p x_1 - b_i x_1 + b_w w_i \\
\dot{x}_2 &= k x_1 - \gamma_p x_2 \\
\dot{w}_i &= b_i x_1 - b_w w_i - \gamma_i w_x \\
\dot{z}_1 &= \mu - \eta z_1 z_2 \\
\dot{z}_2 &= \theta_2 x_2 - \eta z_1 z_2
\end{aligned}$$

where w_i is the buffering species of x_1, and b_i, b_w are the kinetic rates for the buffering reactions. If we assume rapid buffering such that $w_i + x_1$ is the slow variable, $w_i = B_i x_1$ and $B_i = \frac{b_i}{b_w+\gamma_i}$, and use the methodology from SI3 then

$$\begin{aligned}
(1+B_i)\dot{x}_1 &= \theta_1 z_1 - (\gamma_p + B_x\gamma_i)x_1 \\
\dot{x}_2 &= k x_1 - \gamma_p x_2 \\
\dot{z}_1 &= \mu - \eta z_1 z_2 \\
\dot{z}_2 &= \theta_2 x_2 - \eta z_1 z_2.
\end{aligned}$$

Steady State Analysis

We next analyse the steady state. We have

$$\dot{z}_1 - \dot{z}_2 = \mu - \theta_2 x_2$$

and so the steady state of the output is

$$x_2 = \frac{\mu}{\theta_2}.$$

bioRxiv preprint doi: https://doi.org/10.1101/2021.04.18.440372; this version posted April 19, 2021. The copyright holder for this preprint (which was not certified by peer review) is the author/funder, who has granted bioRxiv a license to display the preprint in perpetuity. It is made available under aCC-BY-NC-ND 4.0 International license.

The corresponding steady states of the other species are

$$
\begin{aligned}
x_1 &= \frac{\gamma_p}{k} x_2 = \frac{\gamma_p}{k}\frac{\mu}{\theta_2} \\
z_1 &= \frac{(\gamma_p + B_i\gamma_i)}{\theta_1} x_1 = \frac{\gamma_p^2 \mu}{\theta_1\theta_2 k}\left(1 + B_i\frac{\gamma_i}{\gamma_p}\right) = \frac{\mu}{\alpha}\left(1 + B_i\frac{\gamma_i}{\gamma_p}\right) \\
z_2 &= \frac{1}{\eta}\frac{\mu}{z_1} = \frac{\alpha}{\eta\left(1 + B_i\frac{\gamma_i}{\gamma_p}\right)}
\end{aligned}
$$

where $\alpha = \frac{\theta_1\theta_2 k}{\gamma_p^2}$.

Stability Analysis

We next study the stability of the system. If we linearise about the steady states, we have

$$
\begin{aligned}
(1 + B_i)\Delta\dot{x}_1 &= \theta_1\Delta z_1 - \gamma_p\left(1 + B_i\frac{\gamma_i}{\gamma_p}\right)\Delta x_1 \\
\Delta\dot{x}_2 &= k\Delta x_1 - \gamma_p\Delta x_2 \\
\Delta\dot{z}_1 &= -\eta\bar{z}_2\Delta z_1 - \eta\bar{z}_1\Delta z_2 \\
\Delta\dot{z}_2 &= \theta_2\Delta x_2 - \eta\bar{z}_2\Delta z_1 - \eta\bar{z}_1\Delta z_2.
\end{aligned}
$$

This system can be rewritten as

$$
\begin{aligned}
(1 + B_i)\Delta\dot{x}_1 &= \theta_1\Delta z_1 - \gamma_p\left(1 + B_i\frac{\gamma_i}{\gamma_p}\right)\Delta x_1 \\
\Delta\dot{x}_2 &= k\Delta x_1 - \gamma_p\Delta x_2 \\
\Delta\dot{z}_1 &= -\frac{\alpha}{\left(1 + B_i\frac{\gamma_i}{\gamma_p}\right)}\Delta z_1 - \frac{\beta\left(1 + B_i\frac{\gamma_i}{\gamma_p}\right)}{\alpha}\Delta z_2 \\
\Delta\dot{z}_2 &= \theta_2\Delta x_2 - \frac{\alpha}{\left(1 + B_i\frac{\gamma_i}{\gamma_p}\right)}\Delta z_1 - \frac{\beta\left(1 + B_i\frac{\gamma_i}{\gamma_p}\right)}{\alpha}\Delta z_2.
\end{aligned}
$$

where $\alpha = \frac{\theta_1\theta_2 k}{\gamma_p^2}$ and $\beta = \eta\mu$. Taking the Laplace transforms, we have

$$
\begin{aligned}
&(1 + B_i)\left(s + \frac{\gamma_p + B_i\gamma_i}{1 + B_i}\right)X_1 = \theta_1 Z_1 \\
&(s + \gamma_p)X_2 = kX_1 \\
&\left(s + \frac{\alpha}{\left(1 + B_i\frac{\gamma_i}{\gamma_p}\right)}\right)Z_1 = -\frac{\beta\left(1 + B_i\frac{\gamma_i}{\gamma_p}\right)}{\alpha}Z_2 \\
&\left(s + \frac{\beta\left(1 + B_i\frac{\gamma_i}{\gamma_p}\right)}{\alpha}\right)Z_2 = \theta_2 X_2 - \frac{\alpha}{\left(1 + B_i\frac{\gamma_i}{\gamma_p}\right)}Z_1
\end{aligned}
$$

where $Z_1 = \mathcal{L}\{\Delta z_1\}$, $Z_2 = \mathcal{L}\{\Delta z_2\}$, $X_1 = \mathcal{L}\{\Delta x_1\}$, $X_2 = \mathcal{L}\{\Delta x_2\}$ are the Laplace transforms of the time-domain

bioRxiv preprint doi: https://doi.org/10.1101/2021.04.18.440372; this version posted April 19, 2021. The copyright holder for this preprint (which was not certified by peer review) is the author/funder, who has granted bioRxiv a license to display the preprint in perpetuity. It is made available under aCC-BY-NC-ND 4.0 International license.

concentration deviations. Substituting, we have

$$
\begin{aligned}
&(1+B_i)(s+\gamma_p)\left(s+\frac{\gamma_p+B_i\gamma_i}{1+B_i}\right)X_2=\theta_1 k Z_1\\
&\left(s+\frac{\alpha}{\left(1+B_i\frac{\gamma_i}{\gamma_p}\right)}\right)\left(s+\frac{\beta\left(1+B_i\frac{\gamma_i}{\gamma_p}\right)}{\alpha}\right)Z_1\\
&=-\frac{\beta\left(1+B_i\frac{\gamma_i}{\gamma_p}\right)}{\alpha}\left(\theta_2 X_2-\frac{\alpha}{\left(1+B_i\frac{\gamma_i}{\gamma_p}\right)}Z_1\right).
\end{aligned}
$$

Rewriting and substituting, we have

$$
\begin{aligned}
&(1+B_i)(s+\gamma_p)\left(s+\frac{\gamma_p+B_i\gamma_i}{1+B_i}\right)s\left(s+\frac{\alpha}{\left(1+B_i\frac{\gamma_i}{\gamma_p}\right)}+\frac{\beta\left(1+B_i\frac{\gamma_i}{\gamma_p}\right)}{\alpha}\right)X_2\\
&=-\frac{\beta\left(1+B_i\frac{\gamma_i}{\gamma_p}\right)}{\alpha}\theta_1\theta_2 k X_2.
\end{aligned}
$$

The above equation is equivalent to x_2 buffering (see SI4), and so for strong integral binding we have the stability condition

$$
\gamma_p^3>\frac{\theta_1\theta_2 k}{2+\left(1+\frac{\gamma_i}{\gamma_p}\right)B_i}\frac{1+B_i}{1+\frac{\gamma_i}{\gamma_p}B_i}
$$

which is equivalent to the case of x_2 buffering.

SI5. RAPID x_2 BUFFERING WITH DEGRADATION CAN ENABLE NEAR-PERFECT ADAPTATION DESPITE LEAKY INTEGRATION

In this section, we analyse the ability of buffering at x_2 to enable near perfect adaptation by stabilising antithetic integral feedback. Consider the model (S4) with buffering at x_2 that is degraded

$$
\begin{aligned}
\dot{x}_1&=\theta_1 z_1-\gamma_p x_1\\
\dot{x}_2&=k x_1-\gamma_p x_2-b_x x_2+b_w w_x\\
\dot{w}_x&=b_x x_2-b_w w_x-\gamma_x w_x\\
\dot{z}_1&=\mu-\eta z_1 z_2-\gamma_c z_1\\
\dot{z}_2&=\theta_2 x_2-\eta z_1 z_2-\gamma_c z_2
\end{aligned}
$$

where w_x is the buffering species of x_2, and b_x, b_w are the kinetic rates for the buffering reactions. Using the methodology from SI1 and SI2, we have the reduced model

$$
\begin{aligned}
\dot{x}_1&=\theta_1 z_1-\gamma_p x_1\\
(1+B_x)\dot{x}_2&=k x_1-(\gamma_p+B_x\gamma_x)x_2\\
\dot{z}_1&=\mu-\eta z_1 z_2-\gamma_c z_1\\
\dot{z}_2&=\theta_2 x_2-\eta z_1 z_2-\gamma_c z_2.
\end{aligned}
\tag{S11}
$$

Steady State Analysis

We next analyse the steady state. We have

$$
\dot{z}_1-\dot{z}_2=\mu-\theta_2 x_2-\gamma_c z_1+\gamma_c z_2
$$

bioRxiv preprint doi: https://doi.org/10.1101/2021.04.18.440372; this version posted April 19, 2021. The copyright holder for this preprint (which was not certified by peer review) is the author/funder, who has granted bioRxiv a license to display the preprint in perpetuity. It is made available under aCC-BY-NC-ND 4.0 International license.

and so the steady state of the output is

$$x_2 = \frac{\mu}{\theta_2} - \frac{\gamma_c}{\theta_2} z_1 + \frac{\gamma_c}{\theta_2} z_2.$$

We also have the steady state

$$z_2 = \frac{1}{\eta}\left(\frac{\mu}{z_1} - \gamma_c\right)$$

and so

$$x_2 = \frac{\mu}{\theta_2} - \frac{\gamma_c^2}{\theta_2 \eta} - \frac{\gamma_c}{\theta_2} z_1 + \frac{\gamma_c \mu}{\theta_2 \eta}\frac{1}{z_1}.$$

The other species have the steady states

$$\begin{aligned} x_1 &= \frac{\gamma_p}{k}\left(1 + B_x \frac{\gamma_x}{\gamma_p}\right) x_2 \\ z_1 &= \frac{\gamma_p}{\theta_1} x_1 = \frac{\gamma_p^2}{\theta_1 k}\left(1 + B_x \frac{\gamma_x}{\gamma_p}\right) x_2 = \frac{\theta_2}{\alpha}\left(1 + B_x \frac{\gamma_x}{\gamma_p}\right) x_2 \end{aligned}$$

where $\alpha = \frac{\theta_1 \theta_2 k}{\gamma_p^2}$. Substituting, we have

$$\left(1 + \frac{\gamma_c}{\alpha}\left(1 + B_x \frac{\gamma_x}{\gamma_p}\right)\right) x_2^2 = \left(\frac{\mu}{\theta_2} - \frac{\gamma_c^2}{\theta_2 \eta}\right) x_2 + \frac{\gamma_c \mu \alpha}{\theta_2^2 \eta \left(1 + B_x \frac{\gamma_x}{\gamma_p}\right)}. \tag{S12}$$

We assume strong binding of the sequestration mechanism in antithetic integral feedback (η large), which for steady state is the condition

$$\beta \gg \frac{\gamma_c^2}{\mu}, \frac{\gamma_c \mu \alpha}{\theta_2^2 \left(1 + B_x \frac{\gamma_x}{\gamma_p}\right)}.$$

With this assumption, we have

$$\left(1 + \frac{\gamma_c}{\alpha}\left(1 + B_x \frac{\gamma_x}{\gamma_p}\right)\right) x_2^2 = \frac{\mu}{\theta_2} x_2.$$

We ignore the zero solution, which corresponds to a negative solution in (S12), and so the steady state concentrations are

$$\boxed{x_2 = \frac{\mu}{\theta_2} \frac{1}{1 + \frac{\gamma_c}{\alpha}\left(1 + B_x \frac{\gamma_x}{\gamma_p}\right)}}$$

$$x_1 = \frac{\gamma_p}{k}\frac{\mu}{\theta_2}\frac{\left(1 + B_x \frac{\gamma_x}{\gamma_p}\right)}{1 + \frac{\gamma_c}{\alpha}\left(1 + B_x \frac{\gamma_x}{\gamma_p}\right)}, \quad z_1 = \frac{\mu\left(1 + B_x \frac{\gamma_x}{\gamma_p}\right)}{\alpha + \gamma_c\left(1 + B_x \frac{\gamma_x}{\gamma_p}\right)}, \quad z_2 = \frac{\alpha}{\eta\left(1 + B_x \frac{\gamma_x}{\gamma_p}\right)}.$$

The steady state error of x_2 is

$$\boxed{\frac{x_{2n} - x_2}{x_{2n}} = \frac{1}{1 + \Omega_x}, \quad \Omega_x = \frac{\alpha}{\gamma_c\left(1 + B_x \frac{\gamma_x}{\gamma_p}\right)}}.$$

bioRxiv preprint doi: https://doi.org/10.1101/2021.04.18.440372; this version posted April 19, 2021. The copyright holder for this preprint (which was not certified by peer review) is the author/funder, who has granted bioRxiv a license to display the preprint in perpetuity. It is made available under aCC-BY-NC-ND 4.0 International license.

Stability Analysis

We next study the stability of the system. If we linearise (S11) about the steady state, we have

$$\begin{aligned}
\Delta\dot{x}_1 &= \theta_1\Delta z_1 - \gamma_p\Delta x_1 \\
(1+B_x)\Delta\dot{x}_2 &= k\Delta x_1 - \gamma_p\left(1+B_x\frac{\gamma_x}{\gamma_p}\right)\Delta x_2 \\
\Delta\dot{z}_1 &= -\eta\bar{z}_2\Delta z_1 - \eta\bar{z}_1\Delta z_2 - \gamma_c\Delta z_1 \\
\Delta\dot{z}_2 &= \theta_2\Delta x_2 - \eta\bar{z}_2\Delta z_1 - \eta\bar{z}_1\Delta z_2 - \gamma_c\Delta z_2.
\end{aligned}$$

This system can be rewritten as

$$\begin{aligned}
\Delta\dot{x}_1 &= \theta_1\Delta z_1 - \gamma_p\Delta x_1 \\
(1+B_x)\Delta\dot{x}_2 &= k\Delta x_1 - \gamma_p\left(1+B_x\frac{\gamma_x}{\gamma_p}\right)\Delta x_2 \\
\Delta\dot{z}_1 &= -\left(\frac{\alpha}{\left(1+B_x\frac{\gamma_x}{\gamma_p}\right)}+\gamma_c\right)\Delta z_1 - \frac{\beta\left(1+B_x\frac{\gamma_x}{\gamma_p}\right)}{\alpha+\gamma_c\left(1+B_x\frac{\gamma_x}{\gamma_p}\right)}\Delta z_2 \\
\Delta\dot{z}_2 &= \theta_2\Delta x_2 - \frac{\alpha}{\left(1+B_x\frac{\gamma_x}{\gamma_p}\right)}\Delta z_1 - \left(\frac{\beta\left(1+B_x\frac{\gamma_x}{\gamma_p}\right)}{\alpha+\gamma_c\left(1+B_x\frac{\gamma_x}{\gamma_p}\right)}+\gamma_c\right)\Delta z_2
\end{aligned}$$

where $\alpha = \frac{\theta_1\theta_2 k}{\gamma_p^2}$ and $\beta = \eta\mu$. Taking the Laplace transforms, we have

$$\begin{aligned}
&(s+\gamma_p)X_1 = \theta_1 Z_1 \\
&(1+B_x)\left(s+\frac{\gamma_p+B_x\gamma_x}{1+B_x}\right)X_2 = kX_1 \\
&\left(s+\frac{\alpha}{\left(1+B_x\frac{\gamma_x}{\gamma_p}\right)}+\gamma_c\right)Z_1 = -\frac{\beta\left(1+B_x\frac{\gamma_x}{\gamma_p}\right)}{\alpha+\gamma_c\left(1+B_x\frac{\gamma_x}{\gamma_p}\right)}Z_2 \\
&\left(s+\frac{\beta\left(1+B_x\frac{\gamma_x}{\gamma_p}\right)}{\alpha+\gamma_c\left(1+B_x\frac{\gamma_x}{\gamma_p}\right)}+\gamma_c\right)Z_2 = \theta_2 X_2 - \frac{\alpha}{\left(1+B_x\frac{\gamma_x}{\gamma_p}\right)}Z_1
\end{aligned}$$

where X_1, X_1, Z_1 andZ_2 are the Laplace transforms of $\Delta x_1, \Delta x_2, \Delta z_1$ andΔz_2. Substituting, we have

$$\begin{aligned}
&(1+B_x)(s+\gamma_p)\left(s+\frac{\gamma_p+B_x\gamma_x}{1+B_x}\right)X_2 = \theta_1 k Z_1 \\
&\left(s+\frac{\alpha}{\left(1+B_x\frac{\gamma_x}{\gamma_p}\right)}+\gamma_c\right)\left(s+\frac{\beta\left(1+B_x\frac{\gamma_x}{\gamma_p}\right)}{\alpha+\gamma_c\left(1+B_x\frac{\gamma_x}{\gamma_p}\right)}+\gamma_c\right)Z_1 \\
&= -\frac{\beta\left(1+B_x\frac{\gamma_x}{\gamma_p}\right)}{\alpha+\gamma_c\left(1+B_x\frac{\gamma_x}{\gamma_p}\right)}\left(\theta_2 X_2 - \frac{\alpha}{\left(1+B_x\frac{\gamma_x}{\gamma_p}\right)}Z_1\right).
\end{aligned}$$

Rewriting and substituting, we have

$$\begin{aligned}
&(1+B_x)(s+\gamma_p)\left(s+\frac{\gamma_p+B_x\gamma_x}{1+B_x}\right)\left[(s+\gamma_c)\left(s+\frac{\alpha}{\left(1+B_x\frac{\gamma_x}{\gamma_p}\right)}+\frac{\beta\left(1+B_x\frac{\gamma_x}{\gamma_p}\right)}{\alpha+\gamma_c\left(1+B_x\frac{\gamma_x}{\gamma_p}\right)}+\gamma_c\right)\right]X_2 \\
&= -\frac{\beta\left(1+B_x\frac{\gamma_x}{\gamma_p}\right)}{\alpha+\gamma_c\left(1+B_x\frac{\gamma_x}{\gamma_p}\right)}\theta_1\theta_2 k X_2.
\end{aligned}$$

bioRxiv preprint doi: https://doi.org/10.1101/2021.04.18.440372; this version posted April 19, 2021. The copyright holder for this preprint (which was not certified by peer review) is the author/funder, who has granted bioRxiv a license to display the preprint in perpetuity. It is made available under aCC-BY-NC-ND 4.0 International license.

Simplifying and taking the limit of strong binding of the sequestration mechanism in antithetic integral feedback

$$\beta \gg \frac{\left(\alpha+\gamma_c\left(1+B_x\frac{\gamma_x}{\gamma_p}\right)\right)^2}{\left(1+B_x\frac{\gamma_x}{\gamma_p}\right)^2}, \frac{(\alpha+\gamma_c(1+B_x\frac{\gamma_x}{\gamma_p}))\gamma_p}{\left(1+B_x\frac{\gamma_x}{\gamma_p}\right)}$$

then

$$(1+B_x)(s+\gamma_p)\left(s+\frac{\gamma_p+B_x\gamma_x}{1+B_x}\right)(s+\gamma_c)\left(s+\frac{\beta\left(1+B_x\frac{\gamma_x}{\gamma_p}\right)}{\alpha+\gamma_c\left(1+B_x\frac{\gamma_x}{\gamma_p}\right)}\right)X_2$$
$$=-\frac{\beta\left(1+B_x\frac{\gamma_x}{\gamma_p}\right)}{\alpha+\gamma_c\left(1+B_x\frac{\gamma_x}{\gamma_p}\right)}\theta_1\theta_2 k X_2.$$

Thus we have the characteristic equation

$$(1+B_x)(s+\gamma_p)\left(s+\frac{\gamma_p+B_x\gamma_x}{1+B_x}\right)(s+\gamma_c)\left(s+\frac{\beta\left(1+B_x\frac{\gamma_x}{\gamma_p}\right)}{\alpha+\gamma_c\left(1+B_x\frac{\gamma_x}{\gamma_p}\right)}\right)+\beta\gamma_p^2\frac{\alpha\left(1+B_x\frac{\gamma_x}{\gamma_p}\right)}{\alpha+\gamma_c\left(1+B_x\frac{\gamma_x}{\gamma_p}\right)}=0.$$

Substituting $s=\gamma_p\sigma$, we have

$$(1+B_x)(1+\sigma)\left(\sigma+\frac{1+B_x\frac{\gamma_x}{\gamma_p}}{1+B_x}\right)\left(\sigma+\frac{\gamma_c}{\gamma_p}\right)\left(\sigma+\frac{\beta\left(1+B_x\frac{\gamma_x}{\gamma_p}\right)}{\gamma_p\left(\alpha+\gamma_c\left(1+B_x\frac{\gamma_x}{\gamma_p}\right)\right)}\right)=-\frac{\beta}{\gamma_p^2}\frac{\alpha\left(1+B_x\frac{\gamma_x}{\gamma_p}\right)}{\alpha+\gamma_c\left(1+B_x\frac{\gamma_x}{\gamma_p}\right)}.$$

Using the same argument as that used in SI2, for the stability boundary with strong binding there is a negative real and complex pair of roots in the region $|\sigma| \ll \frac{\beta\left(1+B_x\frac{\gamma_x}{\gamma_p}\right)}{\gamma_p\left(\alpha+\gamma_c\left(1+B_x\frac{\gamma_x}{\gamma_p}\right)\right)}$, as well as one large negative root.

To determine the boundary of stability, we next determine the conditions for which the roots are purely imaginary. Substituting $s=i\omega\gamma_p$, we have

$$(1+B_x)(1+i\omega)\left(i\omega+\frac{1+B_x\frac{\gamma_x}{\gamma_p}}{1+B_x}\right)\left(i\omega+\frac{\gamma_c}{\gamma_p}\right)\left(i\omega+\frac{\beta\left(1+B_x\frac{\gamma_x}{\gamma_p}\right)}{\gamma_p\left(\alpha+\gamma_c\left(1+B_x\frac{\gamma_x}{\gamma_p}\right)\right)}\right)=-\frac{\beta}{\gamma_p^2}\frac{\alpha\left(1+B_x\frac{\gamma_x}{\gamma_p}\right)}{\alpha+\gamma_c\left(1+B_x\frac{\gamma_x}{\gamma_p}\right)}.$$

Taking the strong binding limit where $|i\omega| \ll \frac{\beta\left(1+B_x\frac{\gamma_x}{\gamma_p}\right)}{\gamma_p\left(\alpha+\gamma_c\left(1+B_x\frac{\gamma_x}{\gamma_p}\right)\right)}$, we have

$$(1+i\omega)\left(i\omega+\frac{1+B_x\frac{\gamma_x}{\gamma_p}}{1+B_x}\right)\left(i\omega+\frac{\gamma_c}{\gamma_p}\right)=-\frac{\alpha}{\gamma_p(1+B_x)}.$$

The phase and magnitude constraints are

$$(1+\omega^2)^{0.5}\left(\omega^2+\left(\frac{1+B_x\frac{\gamma_x}{\gamma_p}}{1+B_x}\right)^2\right)^{0.5}\left(\omega^2+\frac{\gamma_c^2}{\gamma_p^2}\right)^{0.5}=\frac{\alpha}{\gamma_p(1+B_x)}$$
$$\tan^{-1}(\omega)+\tan^{-1}\left(\frac{1+B_x}{1+B_x\frac{\gamma_x}{\gamma_p}}\omega\right)+\tan^{-1}\left(\frac{\gamma_p}{\gamma_c}\omega\right)=\pi+2k\pi$$

for some integer k. Solving the phase constraint, we have

$$\tan^{-1}\left(\frac{(1+A^{-1})\omega+\frac{\gamma_p}{\gamma_c}\omega(1-A^{-1}\omega^2)}{1-\left(A^{-1}+(1+A^{-1})\frac{\gamma_p}{\gamma_c}\right)\omega^2}\right)=\pi+2k\pi$$
$$A=\frac{1+B_x\frac{\gamma_x}{\gamma_p}}{1+B_x}.$$

bioRxiv preprint doi: https://doi.org/10.1101/2021.04.18.440372; this version posted April 19, 2021. The copyright holder for this preprint (which was not certified by peer review) is the author/funder, who has granted bioRxiv a license to display the preprint in perpetuity. It is made available under aCC-BY-NC-ND 4.0 International license.

For this we require

$$(1+A^{-1})\omega + \frac{\gamma_p}{\gamma_c}\omega(1-A^{-1}\omega^2) = 0$$

which reduces to

$$\omega^2 = \frac{\gamma_c}{\gamma_p}(1+A) + A.$$

Substituting into the magnitude equation, we have

$$\begin{aligned}
&\left(\left(1+\frac{\gamma_c}{\gamma_p}\right)(1+A)\right)^{0.5}\left(\left(\frac{\gamma_c}{\gamma_p}+A\right)(1+A)\right)^{0.5}\left(\left(\frac{\gamma_c}{\gamma_p}+1\right)\left(\frac{\gamma_c}{\gamma_p}+A\right)\right)^{0.5}\\
&= \left(1+\frac{\gamma_c}{\gamma_p}\right)(1+A)\left(\frac{\gamma_c}{\gamma_p}+A\right)\\
&= \frac{\alpha}{\gamma_p(1+B_x)}.
\end{aligned}$$

Simplifying, we have

$$\frac{\alpha}{\gamma_p(1+B_x)} = \left(1+\frac{\gamma_c}{\gamma_p}\right)(1+A)\left(\frac{\gamma_c}{\gamma_p}+A\right).$$

Multiplying by $A^{-1}\frac{\gamma_p}{\gamma_c}$, we have

$$\begin{aligned}
\frac{\alpha}{\gamma_c\left(1+B_x\frac{\gamma_x}{\gamma_p}\right)} &= A^{-1}\frac{\gamma_p}{\gamma_c}\left(1+\frac{\gamma_c}{\gamma_p}\right)(1+A)\left(\frac{\gamma_c}{\gamma_p}+A\right)\\
A &= \frac{1+B_x\frac{\gamma_x}{\gamma_p}}{1+B_x}.
\end{aligned}$$

and so the stability condition is

$$\boxed{\Omega_x < \left(1+\frac{\gamma_c}{\gamma_p}\right)(1+A)\left(\frac{\gamma_p}{\gamma_c}+A^{-1}\right)}$$

$$\boxed{A = \frac{1+B_x\frac{\gamma_x}{\gamma_p}}{1+B_x}}$$

where

$$\Omega_x = \frac{\alpha}{\gamma_c\left(1+B_x\frac{\gamma_x}{\gamma_p}\right)}.$$

From earlier, we know that the steady state error of x_2 is

$$\frac{x_{2n}-x_2}{x_{2n}} = \frac{1}{1+\Omega_x}.$$

SI6. RAPID x_1 BUFFERING WITH DEGRADATION CAN ENABLE NEAR-PERFECT ADAPTATION DESPITE LEAKY INTEGRATION

In this section, we analyse the ability of buffering at x_1 to enable near perfect adaptation by stabilising antithetic integral feedback. This section uses identical methodology and obtains equivalent results to SI5.

bioRxiv preprint doi: https://doi.org/10.1101/2021.04.18.440372; this version posted April 19, 2021. The copyright holder for this preprint (which was not certified by peer review) is the author/funder, who has granted bioRxiv a license to display the preprint in perpetuity. It is made available under aCC-BY-NC-ND 4.0 International license.

Consider the model with x_1 buffering and dilution

$$\begin{aligned}\dot{x}_1 &= \theta_1 z_1 - \gamma_p x_1 - b_i x_1 + b_w w_x \\ \dot{x}_2 &= k x_1 - \gamma_p x_2 \\ \dot{w}_x &= b_i x_1 - b_w w_x - \gamma_i w_x \\ \dot{z}_1 &= \mu - \eta z_1 z_2 \\ \dot{z}_2 &= \theta_2 x_2 - \eta z_1 z_2\end{aligned}$$

where w_x is the buffering species of x_1, and b_i, b_w are the kinetic rates for the buffering reactions. Assuming rapid buffering and using the same methodology as previous sections, the reduced model is

$$\begin{aligned}(1+B_i)\dot{x}_1 &= \theta_1 z_1 - (\gamma_p + B_i\gamma_i) x_1 \\ \dot{x}_2 &= k x_1 - \gamma_p x_2 \\ \dot{z}_1 &= \mu - \eta z_1 z_2 - \gamma_c z_1 \\ \dot{z}_2 &= \theta_2 x_2 - \eta z_1 z_2 - \gamma_c z_2.\end{aligned}$$

where $B_i = \frac{b_i}{b_w + \gamma_i}$ is the buffer equilibrium ratio.

Steady State Analysis

We next analyse the steady state of the system. We have

$$\dot{z}_1 - \dot{z}_2 = \mu - \theta_2 x_2 - \gamma_c z_1 + \gamma_c z_2$$

and so the steady state of the output is

$$x_2 = \frac{\mu}{\theta_2} - \frac{\gamma_c}{\theta_2} z_1 + \frac{\gamma_c}{\theta_2} z_2.$$

We also have the steady state

$$z_2 = \frac{1}{\eta}\left(\frac{\mu}{z_1} - \gamma_c\right)$$

and so

$$x_2 = \frac{\mu}{\theta_2} - \frac{\gamma_c^2}{\theta_2 \eta} - \frac{\gamma_c}{\theta_2} z_1 + \frac{\gamma_c \mu}{\theta_2 \eta}\frac{1}{z_1}.$$

Now at steady state we have

$$\begin{aligned}x_1 &= \frac{\gamma_p}{k} x_2 \\ z_1 &= \frac{\gamma_p}{\theta_1}\left(1 + B_i\frac{\gamma_i}{\gamma_p}\right) x_1 = \frac{\gamma_p^2}{\theta_1 k}\left(1 + B_i\frac{\gamma_i}{\gamma_p}\right) x_2 = \frac{\theta_2}{\alpha}\left(1 + B_i\frac{\gamma_i}{\gamma_p}\right) x_2\end{aligned}$$

where $\alpha = \frac{\theta_1\theta_2 k}{\gamma_p^2}$. Substituting, we have

$$\left(1 + \frac{\gamma_c}{\alpha}\left(1 + B_i\frac{\gamma_i}{\gamma_p}\right)\right) x_2^2 = \left(\frac{\mu}{\theta_2} - \frac{\gamma_c^2}{\theta_2\eta}\right) x_2 + \frac{\gamma_c \mu \alpha}{\theta_2^2 \eta\left(1 + B_i\frac{\gamma_i}{\gamma_p}\right)}.$$

Assuming strong binding

$$\eta \gg \frac{\gamma_c^2}{\mu}, \frac{\gamma_c \mu \alpha}{\theta_2^2\left(1 + B_i\frac{\gamma_i}{\gamma_p}\right)}$$

bioRxiv preprint doi: https://doi.org/10.1101/2021.04.18.440372; this version posted April 19, 2021. The copyright holder for this preprint (which was not certified by peer review) is the author/funder, who has granted bioRxiv a license to display the preprint in perpetuity. It is made available under aCC-BY-NC-ND 4.0 International license.

we have

$$\left(1+\frac{\gamma_c}{\alpha}\left(1+B_i\frac{\gamma_i}{\gamma_p}\right)\right)x_2^2=\frac{\mu}{\theta_2}x_2$$

and so, ignoring the solution $x_1=0$, the steady state is

$$x_2=\frac{\mu}{\theta_2}\frac{1}{1+\frac{\gamma_c}{\alpha}\left(1+B_i\frac{\gamma_i}{\gamma_p}\right)}$$

$$x_1=\frac{\gamma_p}{k}\frac{\mu}{\theta_2}\frac{1}{1+\frac{\gamma_c}{\alpha}\left(1+B_i\frac{\gamma_i}{\gamma_p}\right)},\quad z_1=\frac{\mu\left(1+B_i\frac{\gamma_i}{\gamma_p}\right)}{\alpha+\gamma_c\left(1+B_i\frac{\gamma_i}{\gamma_p}\right)},\quad z_2=\frac{\alpha}{\eta\left(1+B_i\frac{\gamma_i}{\gamma_p}\right)}.$$

The steady state error of x_2 is

$$\frac{x_{2n}-x_2}{x_{2n}}=\frac{1}{1+\frac{\alpha}{\gamma_c\left(1+B_i\frac{\gamma_i}{\gamma_p}\right)}}.$$

Stability Analysis

We next study the stability of the system. If we linearise about the steady state, we have

$$\begin{aligned}(1+B_i)\Delta\dot{x}_1&=\theta_1\Delta z_1-\gamma_p\left(1+B_i\frac{\gamma_i}{\gamma_p}\right)\Delta x_1\\ \Delta\dot{x}_2&=k\Delta x_1-\gamma_p\Delta x_2\\ \Delta\dot{z}_1&=-\eta\bar{z}_2\Delta z_1-\eta\bar{z}_1\Delta z_2-\gamma_c\Delta z_1\\ \Delta\dot{z}_2&=\theta_2\Delta x_2-\eta\bar{z}_2\Delta z_1-\eta\bar{z}_1\Delta z_2-\gamma_c\Delta z_2.\end{aligned}$$

This system can be rewritten as

$$\begin{aligned}\Delta\dot{x}_1&=\theta_1\Delta z_1-\gamma_p\Delta x_1\\ (1+B_i)\Delta\dot{x}_2&=k\Delta x_1-\gamma_p\left(1+B_i\frac{\gamma_i}{\gamma_p}\right)\Delta x_2\\ \Delta\dot{z}_1&=-\left(\frac{\alpha}{\left(1+B_i\frac{\gamma_i}{\gamma_p}\right)}+\gamma_c\right)\Delta z_1-\frac{\beta\left(1+B_i\frac{\gamma_i}{\gamma_p}\right)}{\alpha+\gamma_c\left(1+B_i\frac{\gamma_i}{\gamma_p}\right)}\Delta z_2\\ \Delta\dot{z}_2&=\theta_2\Delta x_2-\frac{\alpha}{\left(1+B_i\frac{\gamma_i}{\gamma_p}\right)}\Delta z_1-\left(\frac{\beta\left(1+B_i\frac{\gamma_i}{\gamma_p}\right)}{\alpha+\gamma_c\left(1+B_i\frac{\gamma_i}{\gamma_p}\right)}+\gamma_c\right)\Delta z_2.\end{aligned}$$

where $\alpha=\frac{\theta_1\theta_2k}{\gamma_p^2}$ and $\beta=\eta\mu$. Taking the Laplace transforms, we have

$$\begin{aligned}&(1+B_i)\left(s+\frac{\gamma_p+B_i\gamma_i}{1+B_i}\right)X_1=\theta_1Z_1\\ &(s+\gamma_p)X_2=kX_1\\ &\left(s+\frac{\alpha}{\left(1+B_i\frac{\gamma_i}{\gamma_p}\right)}+\gamma_c\right)Z_1=-\frac{\beta\left(1+B_i\frac{\gamma_i}{\gamma_p}\right)}{\alpha+\gamma_c\left(1+B_i\frac{\gamma_i}{\gamma_p}\right)}Z_2\\ &\left(s+\frac{\beta\left(1+B_i\frac{\gamma_i}{\gamma_p}\right)}{\alpha+\gamma_c\left(1+B_i\frac{\gamma_i}{\gamma_p}\right)}+\gamma_c\right)Z_2=\theta_2X_2-\frac{\alpha}{\left(1+B_i\frac{\gamma_i}{\gamma_p}\right)}Z_1.\end{aligned}$$

bioRxiv preprint doi: https://doi.org/10.1101/2021.04.18.440372; this version posted April 19, 2021. The copyright holder for this preprint (which was not certified by peer review) is the author/funder, who has granted bioRxiv a license to display the preprint in perpetuity. It is made available under aCC-BY-NC-ND 4.0 International license.

where X_1, X_2, Z_1 and Z_2 are the Laplace transforms for $\Delta x_1, \Delta x_2, \Delta z_1$ and Δz_2. Substituting, we have

$$(1+B_i)(s+\gamma_p)\left(s+\frac{\gamma_p+B_i\gamma_i}{1+B_i}\right)X_2=\theta_1 k Z_1$$

$$\left(s+\frac{\alpha}{\left(1+B_i\frac{\gamma_i}{\gamma_p}\right)}+\gamma_c\right)\left(s+\frac{\beta\left(1+B_i\frac{\gamma_i}{\gamma_p}\right)}{\alpha+\gamma_c\left(1+B_i\frac{\gamma_i}{\gamma_p}\right)}+\gamma_c\right)Z_1$$

$$=-\frac{\beta\left(1+B_i\frac{\gamma_i}{\gamma_p}\right)}{\alpha+\gamma_c\left(1+B_i\frac{\gamma_i}{\gamma_p}\right)}\left(\theta_2 X_2-\frac{\alpha}{\left(1+B_i\frac{\gamma_i}{\gamma_p}\right)}Z_1\right).$$

Rewriting and substituting, we have

$$(1+B_i)(s+\gamma_p)\left(s+\frac{\gamma_p+B_i\gamma_i}{1+B_i}\right)\left[(s+\gamma_c)\left(s+\frac{\alpha}{\left(1+B_i\frac{\gamma_i}{\gamma_p}\right)}+\frac{\beta\left(1+B_i\frac{\gamma_i}{\gamma_p}\right)}{\alpha+\gamma_c\left(1+B_i\frac{\gamma_i}{\gamma_p}\right)}+\gamma_c\right)\right]X_2$$

$$=-\frac{\beta\left(1+B_i\frac{\gamma_i}{\gamma_p}\right)}{\alpha+\gamma_c\left(1+B_i\frac{\gamma_i}{\gamma_p}\right)}\theta_1\theta_2 k X_2$$

The above equation is equivalent to that for x_2 buffering (see SI5), and so for strong integral binding we have the equivalent stability constraint and steady state error

$$\frac{x_{2n}-x_2}{x_{2n}}=\frac{1}{1+\Omega_i}$$

$$\Omega_i<\left(1+\frac{\gamma_c}{\gamma_p}\right)(1+A)\left(\frac{\gamma_p}{\gamma_c}+A^{-1}\right)$$

$$A=\frac{1+\frac{\gamma_i}{\gamma_p}B_i}{1+B_i}.$$

SI7. RAPID z_1 BUFFERING WITH DEGRADATION HAS A TRADE-OFF DUE TO LEAKY INTEGRATION

In this section, we analyse the trade-offs for rapid buffering at z_1 on stability and the steady state error from perfect adaptation. For buffering at z_1 with dilution, we use the model

$$\begin{aligned}\dot{x}_1&=\theta_1 z_1-\gamma_p x_1\\ \dot{x}_2&=kx_1-\gamma_p x-\gamma_p x_2\\ \dot{z}_1&=\mu-\eta z_1 z_2-\gamma_c z_1-b_1 z_1+b_w w\\ \dot{z}_2&=\theta_2 x_2-\eta z_1 z_2-\gamma_c z_2\\ \dot{w}&=b_1 z_1-b_w w-\gamma_c w\end{aligned}$$

where x_2 is the output concentration being controlled, x_1 is another concentration in the process being controlled, and z_1 and z_2 represent the molecular species involved in the perfect adaptation mechanism. Assuming that the buffer is rapid then w is at quasi-steady state then

$$w=B_1 z_1 \quad B_1=\frac{b_1}{b_w+\gamma_c}.$$

If $x_T=w+z_1$ is the slow variable then $x_T=(1+B_1)z_1$. Thus $\dot{x}_T=(1+B_1)\dot{z}_1$ and so

$$(1+B_1)\dot{z}_1=\mu-\eta z_1 z_2-\gamma_c(1+B_1)z_1.$$

Thus we have

$$\begin{aligned}\dot{x}_1&=\theta_1 z_1-\gamma_p x_1\\ \dot{x}_2&=kx_1-\gamma_p x_2\\ (1+B_1)\dot{z}_1&=\mu-\eta z_1 z_2-\gamma_c(1+B_1)z_1\\ \dot{z}_2&=\theta_2 x_2-\eta z_1 z_2-\gamma_c z_2.\end{aligned}$$

bioRxiv preprint doi: https://doi.org/10.1101/2021.04.18.440372; this version posted April 19, 2021. The copyright holder for this preprint (which was not certified by peer review) is the author/funder, who has granted bioRxiv a license to display the preprint in perpetuity. It is made available under aCC-BY-NC-ND 4.0 International license.

Steady State Analysis

We next determine the steady state and and any error from perfect adaptation. For the case of dilution, we have

$$(1+B_1)\dot{z}_1 - \dot{z}_2 = \mu - \theta_2 x_2 - \gamma_c((1+B_1)z_1 - z_2) = 0$$

resulting in

$$x_2 = \frac{\mu}{\theta_2} - \frac{\gamma_c}{\theta_2}(1+B_1)z_1 + \frac{\gamma_c}{\theta_2}z_2.$$

We also have

$$z_2 = \frac{1}{\eta}\left(\frac{\mu}{z_1} - \gamma_c(1+B_1)\right)$$

and so

$$x_2 = \frac{\mu}{\theta_2} - \frac{\gamma_c^2}{\theta_2\eta}(1+B_1) - \frac{\gamma_c}{\theta_2}(1+B_1)z_1 + \frac{\gamma_c\mu}{\theta_2\eta}\frac{1}{z_1}.$$

Now at steady state we have

$$x_1 = \frac{\gamma_p}{k}x_2$$
$$z_1 = \frac{\gamma_p}{\theta_1}x_1 = \frac{\gamma_p^2}{\theta_1 k}x_2 = \frac{\theta_2}{\alpha}x_2.$$

where $\alpha = \frac{\theta_1\theta_2 k}{\gamma_p^2}$. Substituting, we have

$$\left(1 + \frac{\gamma_c}{\alpha}(1+B_1)\right)x_2^2 = \left(\frac{\mu}{\theta_2} - \frac{\gamma_c^2}{\theta_2\eta}(1+B_1)\right)x_2 + \frac{\gamma_c\mu\alpha}{\theta_2^2\eta}.$$

Assuming strong binding of the sequestration mechanism

$$\eta \gg \frac{\gamma_c^2(1+B_1)}{\mu}, \frac{\gamma_c\mu\alpha}{\theta_2^2}$$

we have

$$\left(1 + \frac{\gamma_c}{\alpha}(1+B_1)\right)x_2^2 = \frac{\mu}{\theta_2}x_2$$

and so, ignoring the zero solution, the steady state is

$$\boxed{x_2 = \frac{\mu}{\theta_2}\frac{1}{1+\frac{\gamma_c}{\alpha}(1+B_1)}} \tag{S13}$$

$$x_1 = \frac{\gamma_p}{k}\frac{\mu}{\theta_2}\frac{1}{1+\frac{\gamma_c}{\alpha}(1+B_1)}, \quad z_1 = \frac{\mu}{\alpha+\gamma_c(1+B_1)}, \quad z_2 = \frac{\alpha}{\eta}. \tag{S14}$$

The steady state error of x_2 is

$$\boxed{\frac{x_{2n}-x_2}{x_{2n}} = \frac{1}{1+\Omega_1}, \quad \Omega_1 = \frac{\alpha}{\gamma_c(1+B_1)}}.$$

We can see that increasing B_1 increases the steady state error of x_2 when there is degradation/dilution of z_1 and z_2.

bioRxiv preprint doi: https://doi.org/10.1101/2021.04.18.440372; this version posted April 19, 2021. The copyright holder for this preprint (which was not certified by peer review) is the author/funder, who has granted bioRxiv a license to display the preprint in perpetuity. It is made available under aCC-BY-NC-ND 4.0 International license.

Stability Analysis

We next study the stability of the system with degradation. If we linearise about the steady states, we have

$$\begin{aligned}
\Delta\dot{x}_1 &= \theta_1\Delta z_1 - \gamma_p\Delta x_1 \\
\Delta\dot{x}_2 &= k\Delta x_1 - \gamma_p\Delta x_2 \\
(1+B_1)\Delta\dot{z}_1 &= -\eta\bar{z}_2\Delta z_1 - \eta\bar{z}_1\Delta z_2 - \gamma_c(1+B_1)\Delta z_1 \\
\Delta\dot{z}_2 &= \theta_2\Delta x_2 - \eta\bar{z}_2\Delta z_1 - \eta\bar{z}_1\Delta z_2 - \gamma_c\Delta z_2.
\end{aligned}$$

This system can be rewritten as

$$\begin{aligned}
\Delta\dot{x}_1 &= \theta_1\Delta z_1 - \gamma_p\Delta x_1 \\
\Delta\dot{x}_2 &= k\Delta x_1 - \gamma_p\Delta x_2 \\
(1+B_1)\Delta\dot{z}_1 &= -(\alpha+\gamma_c(1+B_1))\Delta z_1 - \frac{\beta}{\alpha+\gamma_c(1+B_1)}\Delta z_2 \\
\Delta\dot{z}_2 &= \theta_2\Delta x_2 - \alpha\Delta z_1 - \left(\frac{\beta}{\alpha+\gamma_c(1+B_1)} + \gamma_c\right)\Delta z_2
\end{aligned}$$

where

$$\alpha = \frac{\theta_1\theta_2 k}{\gamma_p^2}, \quad \beta = \eta\mu.$$

Taking the Laplace transforms, we have

$$\begin{aligned}
&(s+\gamma_p)X_1 = \theta_1 Z_1 \\
&(s+\gamma_p)X_2 = kX_1 \\
&((1+B_1)s+\alpha+\gamma_c(1+B_1))Z_1 = -\frac{\beta}{\alpha+\gamma_c(1+B_1)}Z_2 \\
&\left(s+\frac{\beta}{\alpha+\gamma_c(1+B_1)}+\gamma_c\right)Z_2 = \theta_2 X_2 - \alpha Z_1.
\end{aligned}$$

where X_1, X_2, Z_1 and Z_2 are the laplace transforms for $\Delta x_1, \Delta x_2, \Delta z_1$ and Δz_2. Substituting, we have

$$\begin{aligned}
&(s+\gamma_p)^2 X_2 = \theta_1 k Z_1 \\
&((1+B_1)s+\alpha+\gamma_c(1+B_1))\left(s+\frac{\beta}{\alpha+\gamma_c(1+B_1)}+\gamma_c\right)Z_1 \\
&= -\frac{\beta}{\alpha+\gamma_c(1+B_1)}(\theta_2 X_2 - \alpha Z_1).
\end{aligned}$$

Rewriting and substituting, we have

$$\begin{aligned}
&(s+\gamma_p)^2\left[(s+\gamma_c)\left((1+B_1)s+\alpha+\frac{\beta(1+B_1)}{\alpha+\gamma_c(1+B_1)}+\gamma_c(1+B_1)\right)\right]X_2 \\
&= -\frac{\beta}{\alpha+\gamma_c(1+B_1)}\theta_1\theta_2 k X_2.
\end{aligned}$$

Taking the limit of strong binding $\left(\beta \gg \max\left\{\frac{(\alpha+\gamma_c(1+B_1))^2}{1+B_1}, \frac{\gamma_p(\alpha+\gamma_c(1+B_1))}{1+B_1}\right\}\right)$ then

$$(1+B_1)(s+\gamma_p)^2(s+\gamma_c)\left(s+\frac{\beta}{\alpha+\gamma_c(1+B_1)}\right)X_2 = -\frac{\beta}{\alpha+\gamma_c(1+B_1)}\theta_1\theta_2 k X_2.$$

Thus we have the characteristic equation

$$(s+\gamma_p)^2(s+\gamma_c)\left(s+\frac{\beta}{\alpha+\gamma_c(1+B_1)}\right) + \frac{\beta\gamma_p^2}{(1+B_1)}\frac{\alpha}{\alpha+\gamma_c(1+B_1)} = 0.$$

bioRxiv preprint doi: https://doi.org/10.1101/2021.04.18.440372; this version posted April 19, 2021. The copyright holder for this preprint (which was not certified by peer review) is the author/funder, who has granted bioRxiv a license to display the preprint in perpetuity. It is made available under aCC-BY-NC-ND 4.0 International license.

Substituting $s = \gamma_p \sigma$, we have

$$(1+\sigma)^2 \left(\sigma + \frac{\gamma_c}{\gamma_p}\right)\left(\sigma + \frac{\beta}{\gamma_p(\alpha+\gamma_c(1+B_1))}\right) = -\frac{\beta}{\gamma_p^2(1+B_1)}\frac{\alpha}{\alpha+\gamma_c(1+B_1)}.$$

Using the same argument as above, for the stability boundary with strong binding there is a negative real and complex pair of roots in the region $|\sigma| \ll \frac{\beta}{\gamma_p(\alpha+\gamma_c(1+B_1))}$, as well as one large negative root.
To determine the boundary of stability, we next determine the conditions for which the roots are purely imaginary. Substituting $s = i\omega\gamma_p$, we have

$$(1+i\omega)^2 \left(i\omega + \frac{\gamma_c}{\gamma_p}\right)\left(i\omega + \frac{\beta}{\gamma_p(\alpha+\gamma_c(1+B_1))}\right) = -\frac{\beta}{\gamma_p^2(1+B_1)}\frac{\alpha}{\alpha+\gamma_c(1+B_1)}.$$

Taking the strong binding limit where $|i\omega| \ll \frac{\beta}{\gamma_p(\alpha+\gamma_c(1+B_1))}$, we have

$$(1+i\omega)^2 \left(i\omega + \frac{\gamma_c}{\gamma_p}\right) = -\frac{\alpha}{\gamma_p(1+B_1)}.$$

The phase and magnitude constraints are

$$(1+\omega^2)\left(\omega^2 + \frac{\gamma_c^2}{\gamma_p^2}\right)^{0.5} = \frac{\alpha}{\gamma_p(1+B_1)}$$
$$2\tan^{-1}(\omega) + \tan^{-1}\left(\frac{\gamma_p}{\gamma_c}\omega\right) = \pi + 2k\pi.$$

for some integer k. Solving the phase constraint, we have

$$\tan^{-1}\left(\frac{2\omega + \frac{\gamma_p}{\gamma_c}\omega(1-\omega^2)}{1-\left(1+2\frac{\gamma_p}{\gamma_c}\right)\omega^2}\right) = \pi + 2k\pi.$$

For this, we require

$$2\omega + \frac{\gamma_p}{\gamma_c}\omega(1-\omega^2)$$

which reduces to

$$\omega = \sqrt{2\frac{\gamma_c}{\gamma_p} + 1}.$$

Substituting into the magnitude equation, we have

$$\frac{\alpha}{\gamma_p(1+B_1)} = 2\left(1+\frac{\gamma_c}{\gamma_p}\right)^2.$$

As a consequence, the stability constraint is

$$\Omega_1 = \frac{\alpha}{\gamma_c(1+B_1)} < 2\frac{\gamma_p}{\gamma_c}\left(1+\frac{\gamma_c}{\gamma_p}\right)^2.$$

We can observe that increasing B_1 improves the stability constraint. However, the steady state error of x_2 is

$$\frac{x_{2n}-x_2}{x_{2n}} = \frac{1}{1+\Omega_1}$$
$$\Omega_1 = \frac{\alpha}{\gamma_c(1+B_1)}$$

$$\boxed{\Omega_1 < 2\frac{\gamma_p}{\gamma_c}\left(1+\frac{\gamma_c}{\gamma_p}\right)^2}$$

Thus there is a steady state error constraint that is independent of B_1, and so increasing B_1 does not enable the removal of leaky integration. This result is a consequence of the added degradation of the buffer, which cancels the stabilising effect of the buffer.

bioRxiv preprint doi: https://doi.org/10.1101/2021.04.18.440372; this version posted April 19, 2021. The copyright holder for this preprint (which was not certified by peer review) is the author/funder, who has granted bioRxiv a license to display the preprint in perpetuity. It is made available under aCC-BY-NC-ND 4.0 International license.

SI8. NON-RAPID BUFFERING CAN ALLOW NEAR PERFECT ADAPTATION WITH LEAKY INTEGRATION

In this section, we analyse the ability of non-rapid buffering at z_1 to enable near perfect adaptation by stabilising antithetic integral feedback. We use the model

$$\begin{aligned}
\dot{x}_1 &= \theta_1 z_1 - \gamma_p x_1 \\
\dot{x}_2 &= k x_1 - \gamma_p x_2 \\
\dot{z}_1 &= \mu - \eta z_1 z_2 - \gamma_c z_1 - b_1 z_1 + b_w w \\
\dot{z}_2 &= \theta_2 x_2 - \eta z_1 z_2 - \gamma_c z_2 \\
\dot{w} &= b_1 z_1 - b_w w - \gamma_c w.
\end{aligned} \tag{S15}$$

where the buffer w is not assumed to rapidly reach equilbrium. As a result, the model cannot be reduced in a similar manner to previous sections. The steady state for (S15) is identical to the rapid case in SI7. The linearisation is

$$\begin{aligned}
\Delta\dot{x}_1 &= \theta_1 \Delta z_1 - \gamma_p \Delta x_1 \\
\Delta\dot{x}_2 &= k \Delta x_1 - \gamma_p \Delta x_2 \\
\Delta\dot{z}_1 &= -\eta \bar{z}_2 \Delta z_1 - \eta \bar{z}_1 \Delta z_2 - \gamma_c \Delta z_1 - b_1 \Delta z_1 + b_w \Delta w \\
\Delta\dot{z}_2 &= \theta_2 \Delta x_2 - \eta \bar{z}_2 \Delta z_1 - \eta \bar{z}_1 \Delta z_2 - \gamma_c \Delta z_2 \\
\Delta\dot{w} &= b_1 \Delta z_1 - (b_w + \gamma_c) \Delta w.
\end{aligned}$$

This system can be rewritten

$$\begin{aligned}
\Delta\dot{x}_1 &= \theta_1 \Delta z_1 - \gamma_p \Delta x_1 \\
\Delta\dot{x}_2 &= k \Delta x_1 - \gamma_p \Delta x_2 \\
\Delta\dot{z}_1 &= -(\alpha + \gamma_c) \Delta z_1 - \frac{\beta}{\alpha + \gamma_c (1 + B_1)} \Delta z_2 - b_1 \Delta z_1 + b_w \Delta w \\
\Delta\dot{z}_2 &= \theta_2 \Delta x_2 - \alpha \Delta z_1 - \left(\frac{\beta}{\alpha + \gamma_c (1 + B_1)} + \gamma_c \right) \Delta z_2 \\
\Delta\dot{w} &= b_1 \Delta z_1 - (b_w + \gamma_c) \Delta w.
\end{aligned}$$

where

$$\alpha = \frac{\theta_1 \theta_2 k}{\gamma_p^2}, \quad \beta = \eta \mu.$$

Taking the Laplace transform of $\Delta\dot{w} = b_1 \Delta z_1 - (b_w + \gamma_c) \Delta w$, we have

$$W = \frac{b_1}{s + b_w + \gamma_c} Z_1$$

where W and Z_1 are the Laplace transforms of w and z_1. We have

$$\begin{aligned}
-b_1 Z_1 + b_w W &= -b_1 Z_1 + b_w \frac{b_1}{s + b_w + \gamma_c} Z_1 \\
&= -B_1 \frac{s + \gamma_c}{1 + \frac{s}{b_w + \gamma_c}} Z_1 \\
&= -C_b(s) Z_1
\end{aligned}$$

where

$$C_b = B_1 \frac{s + \gamma_c}{1 + s\tau}, \quad \tau = \frac{1}{b_w + \gamma_c}.$$

bioRxiv preprint doi: https://doi.org/10.1101/2021.04.18.440372; this version posted April 19, 2021. The copyright holder for this preprint (which was not certified by peer review) is the author/funder, who has granted bioRxiv a license to display the preprint in perpetuity. It is made available under aCC-BY-NC-ND 4.0 International license.

Thus

$$
\begin{aligned}
&(s+\gamma_p)X_1 = \theta_1 Z_1 \\
&(s+\gamma_p)X_2 = kX_1 \\
&(s+\alpha+\gamma_c+C_b)Z_1 = -\frac{\beta}{\alpha+\gamma_c(1+B_1)}Z_2 \\
&\left(s+\frac{\beta}{\alpha+\gamma_c(1+B_1)}+\gamma_c\right)Z_2 = \theta_2 X_2 - \alpha Z_1.
\end{aligned}
$$

Combining, we have

$$
\begin{aligned}
&(s+\gamma_p)^2 X_2 = \theta_1 k Z_1 \\
&(s+\alpha+\gamma_c+C_b)\left(s+\frac{\beta}{\alpha+\gamma_c(1+B_1)}+\gamma_c\right)Z_1 = -\frac{\beta}{\alpha+\gamma_c(1+B_1)}(\theta_2 X_2 - \alpha Z_1).
\end{aligned}
$$

Simplifying, we have

$$
\begin{aligned}
&\left[(s+\gamma_c)\left(s+\alpha+\frac{\beta}{\alpha+\gamma_c(1+B_1)}+\gamma_c\right)+C_b\left(s+\frac{\beta}{\alpha+\gamma_c(1+B_1)}+\gamma_c\right)\right]Z_1 \\
&= -\frac{\beta}{\alpha+\gamma_c(1+B_1)}\theta_2 X_2.
\end{aligned}
$$

Taking the strong binding limit of the sequestration mechanism ($\beta \gg \max\left\{(\alpha+\gamma_c)(\alpha+\gamma_c(1+B_1)), \gamma_p(\alpha+\gamma_c(1+B_1))\right\}$), we have

$$
\begin{aligned}
&(s+\gamma_c+C_b)\left(s+\frac{\beta}{\alpha+\gamma_c(1+B_1)}\right)Z_1 \\
&= -\frac{\beta}{\alpha+\gamma_c(1+B_1)}\theta_2 X_2
\end{aligned}
$$

and so

$$
\begin{aligned}
&(s+\gamma_p)^2\left[(s+\gamma_c+C_b)\left(s+\frac{\beta}{\alpha+\gamma_c(1+B_1)}\right)\right]X_2 \\
&= -\beta\gamma_p^2\frac{\alpha}{\alpha+\gamma_c(1+B_1)}X_2.
\end{aligned}
$$

Rewriting C_b, we have

$$
\left[(s+\gamma_p)^2(s+\gamma_c)\frac{1+B_1+\tau s}{1+\tau s}\left(s+\frac{\beta}{\alpha+\gamma_c(1+B_1)}\right)+\beta\gamma_p^2\frac{\alpha}{\alpha+\gamma_c(1+B_1)}\right]X_2 = 0
$$

or

$$
\left[(s+\gamma_p)^2(s+\gamma_c)(1+B_1+\tau s)\left(s+\frac{\beta}{\alpha+\gamma_c(1+B_1)}\right)+\beta\gamma_p^2\frac{\alpha(1+\tau s)}{\alpha+\gamma_c(1+B_1)}\right]X_2 = 0.
$$

Substituting $s = i\omega\gamma_p$, we have

$$
(1+B_1+i\omega\tau\gamma_p)(1+i\omega)^2\left(\frac{\gamma_c}{\gamma_p}+i\omega\right)\left(i\omega+\frac{\beta}{\gamma_p(\alpha+\gamma_c(1+B_1))}\right)+\frac{\beta}{\gamma_p^2}\frac{\alpha(1+i\omega\tau\gamma_p)}{\alpha+\gamma_c(1+B_1)} = 0.
$$

Taking the strong binding limit where $|i\omega| \ll \frac{\beta}{\gamma_p(\alpha+\gamma_c(1+B_1))}$, we have

$$
(1+B_1+i\omega\tau\gamma_p)(1+i\omega)^2\left(\frac{\gamma_c}{\gamma_p}+i\omega\right) = -\frac{\alpha}{\gamma_p}(1+i\omega\tau\gamma_p).
$$

bioRxiv preprint doi: https://doi.org/10.1101/2021.04.18.440372; this version posted April 19, 2021. The copyright holder for this preprint (which was not certified by peer review) is the author/funder, who has granted bioRxiv a license to display the preprint in perpetuity. It is made available under aCC-BY-NC-ND 4.0 International license.

The magnitude constraint is

$$(1+B_1)\left(1+\frac{\omega^2\tau^2\gamma_p^2}{(1+B_1)^2}\right)^{0.5}(1+\omega^2)\left(\frac{\gamma_c^2}{\gamma_p^2}+\omega^2\right)^{0.5}=\frac{\alpha}{\gamma_p}(1+\omega^2\tau^2\gamma_p^2)^{0.5} \tag{S16}$$

and the phase constraint is

$$2\tan^{-1}(\omega)+\tan^{-1}\left(\frac{\gamma_p}{\gamma_c}\omega\right)-\tan^{-1}\left(\tau\gamma_p\omega\right)+\tan^{-1}\left(\frac{\tau\gamma_p}{1+B_1}\omega\right)=\pi+2k\pi.$$

for some integer k. Using trigonometric identities, we have

$$\tan^{-1}\left(\frac{2\omega+\frac{\gamma_p}{\gamma_c}\omega(1-\omega^2)}{1-\left(1+2\frac{\gamma_p}{\gamma_c}\right)\omega^2}\right)=\pi+2k\pi+\tan^{-1}\left(\frac{\frac{B_1}{1+B_1}\tau\gamma_p\omega}{1+\frac{1}{1+B_1}\tau^2\gamma_p^2\omega^2}\right).$$

This can be simplified to

$$\frac{2\omega+\frac{\gamma_p}{\gamma_c}\omega(1-\omega^2)}{1-\left(1+2\frac{\gamma_p}{\gamma_c}\right)\omega^2}=\frac{\frac{B_1}{1+B_1}\tau\gamma_p\omega}{1+\frac{1}{1+B_1}\tau^2\gamma_p^2\omega^2}.$$

Ignoring the trivial solution $\omega=0$, we have

$$\left(2+\frac{\gamma_p}{\gamma_c}-\frac{\gamma_p}{\gamma_c}\omega^2\right)\left(1+\frac{1}{1+B_1}\tau^2\gamma_p^2\omega^2\right)=\frac{B_1}{1+B_1}\tau\gamma_p\left(1-\left(1+2\frac{\gamma_p}{\gamma_c}\right)\omega^2\right).$$

If for simplicity we assume that B_1 is large, then we have

$$2+\frac{\gamma_p}{\gamma_c}-\frac{\gamma_p}{\gamma_c}\omega^2=\tau\gamma_p-\tau\gamma_p\left(1+2\frac{\gamma_p}{\gamma_c}\right)\omega^2$$

and so

$$\boxed{\omega^2=\frac{1+2\frac{\gamma_c}{\gamma_p}-\tau\gamma_c}{1-\tau\gamma_c\left(1+2\frac{\gamma_p}{\gamma_c}\right)},\quad \tau=\frac{1}{b_w+\gamma_c}}.$$

Thus ω^2 is monotonically increasing wrt τ for $\tau\gamma_c(1+2\frac{\gamma_p}{\gamma_c})<1$.
From the magnitude constraint S16, we have the stability constraint

$$\Omega_1=\frac{\alpha}{\gamma_c(1+B_1)}$$
$$\Omega_1<\frac{\gamma_p}{\gamma_c}\left(\frac{1+\frac{\omega^2\tau^2\gamma_p^2}{(1+B_1)^2}}{1+\omega^2\tau^2\gamma_p^2}\right)^{0.5}(1+\omega^2)\left(\frac{\gamma_c^2}{\gamma_p^2}+\omega^2\right)^{0.5}.$$

We can rewrite Ω_1 as

$$\boxed{\Omega_1<\left(1+\frac{\omega^2\tau^2\gamma_p^2}{(1+B_1)^2}\right)^{0.5}\left(\frac{1+\omega^2\frac{\gamma_p^2}{\gamma_c^2}}{1+\omega^2\tau^2\gamma_p^2}\right)^{0.5}(1+\omega^2)}.$$

We can observe that Ω_1 is monotonically increasing with ω as $\tau=1/(\gamma_c+b_w)<1/\gamma_c$. Combining, Ω_1 is monotonically increasing with respect to τ. Thus increasing τ improves the stability constraint for large B_1. As the steady state error is

$$\frac{x_{2n}-x_2}{x_{2n}}=\frac{1}{1+\Omega_1}$$

then increasing τ decreases the steady state error constraint.

bioRxiv preprint doi: https://doi.org/10.1101/2021.04.18.440372; this version posted April 19, 2021. The copyright holder for this preprint (which was not certified by peer review) is the author/funder, who has granted bioRxiv a license to display the preprint in perpetuity. It is made available under aCC-BY-NC-ND 4.0 International license.

SI9. BODE INTEGRAL OF BUFFERING AND ANTITHETIC INTEGRAL FEEDBACK

Feedback is a highly effective method of robust regulation, but this mechanism is subject to fundamental limits. The Bode integral describes one of these fundamental limit, where improving the regulation at one frequency of a disturbance will worsen regulation of disturbances at other frequencies.
To observe this mathematically, we let $r(t)$ be the reference signal (corresponding to μ). We can mathematically decompose $r(t)$ and $e = r(t) - x_2(t)$ into their 'fast' and 'slow' components (via a Fourier transform), which we write as $R(i\omega)$ and $E(i\omega)$ respectively. A useful measure of regulation is the sensitivity function $S(i\omega) = \frac{E(i\omega)}{R(i\omega)}$.
The model of the system is

$$\begin{aligned}
\dot{x}_1 &= \theta_1 z_1 - \gamma_p x_1 \\
\dot{x}_2 &= k x_1 - \gamma_p x_2 - b_x w + b_x w_x \\
\dot{w}_x &= b_x x - b_w w_x - \gamma_x w \\
\dot{z}_1 &= \mu - \eta z_1 z_2 - \gamma_c z_1 - b_1 z_1 + b_w w_1 \\
\dot{w}_1 &= b_1 z_1 - b_w w_1 - \gamma_c w_1 \\
\dot{z}_2 &= \theta_2 x_2 - \eta z_1 z_2 - \gamma_c z_2.
\end{aligned}$$

We can write the open-loop model of the two state

$$\begin{aligned}
\dot{x}_1 &= \theta_1 u_a - \gamma_p x_1 \\
\dot{x}_2 &= k x_1 - \gamma_p x_2 + u_b
\end{aligned}$$

where u_a is the process input for antithetic integral feedback and u_b is the input for buffering at x_2, and z_1, z_2 and w_x are controller variables.
Buffering at z_1 and antithetic integral feedback act through the input u_a while buffering at x_2 acts through u_b.
The bode integral is a fundamental constraint on the effectiveness of feedback in any system. It provides a constraint on the overall regulatory effectiveness in terms of the sensitivity function. With output buffering, Bode's integral is[16]

$$\int_0^\infty \log\left(|S(i\omega)|\right) d\omega = -\frac{\pi}{2} b_x$$

where the integral of $S(i\omega)$ represents an overall measure of regulation, b_x is the kinetic rate of the forward buffering reaction and it is assumed that the system without feedback is stable. The integral of $S(i\omega)$ sums the regulation of disturbances at different 'speeds'. Without buffering, if regulation is improved at one 'speed' of regulation, it worsens at other 'speeds'. However, increasing b_x reduces the integral. Thus the trade-off does not occur with buffering, which can uniformly improve regulation.
In contrast, control species buffering is part of the feedback regulation mechanism and so Bode's integral is[16]

$$\int_0^\infty \log\left(|S(i\omega)|\right) d\omega = 0.$$

Thus control buffering does not remove fundamental constraints, despite stabilising buffering. The tradeoff remains such that improving regulation at one frequency will worsen regulation of disturbances at other frequencies.